Supplementary Information for

Achieving dual-mode long-persistence afterglow through aromatic furan organic host-guest system

Zheng Gong[a], Qingyang Cui[a], Xiancheng Nie[a], Guoqing Zhang*[a] and Biao Chen*[a]

[a]Hefei National Laboratory for Physical Sciences at the Microscale, University of Science and Technology of China, Hefei, 230026, P. R. China. E-mail: gzhang@ustc.edu.cn; biaochen@ustc.edu.cn

1. Materials and Methods

1.1 Materials

Solvent: 1,4-dioxane (99%, Sinopharm Chemical Reagent Co., Ltd), acetone (99%, Sinopharm Chemical Reagent Co., Ltd), tetrahydrofuran (99%, Macklin), dichloromethane (99%, Macklin), and dried 2-methyltetrahydrofuran (99%, Macklin) refluxed with calcium hydride; Deionized Water was deionized with a Milli-Q SP reagent water system (Millipore) to a specific resistivity of 18.2 MΩ.cm; Deuterated chloroform (99%, Sigma-Aldrich LLC), deuterated dimethyl sulfoxide (99%, Sigma-Aldrich LLC), and HPLC grade acetonitrile (99.9%, Sigma-Aldrich LLC).

Reagents: 2-bromodibenzo [b, d] furan (98%, Bidepharm), 8-bromo-1-chlorodibenzo [b, d] furan (97%, Bidepharm), naphtho [2,1-b] benzofuran (97%, Bidepharm), 10 bromonaphtho [2,1]-b] Benzofuran (98%, Bidepharm) and 2-naphtho [2,1-b:1 ', 2' - d] furan (97%, Bidepharm). Column chromatography and recrystallization were used for all samples prior to luminescence spectral analysis.

1.2 Methods

Instrumentation. NMR spectra were recorded on a Bruker AV400 NMR spectrometer operated in the Fourier transform mode, NMR spectra were recorded at 400 MHz for ^{1}H and 101 MHz for ^{13}C. ^{1}H NMR spectra are represented as follows: chemical shift, multiplicity (s = singlet, d = doublet, t = triplet, q = quartet, m = multiplet, br = broad), integration, and coupling

constant (*J*) in Hertz (Hz). ^{1}H NMR spectra were referenced to the signal for residual protio chloroform at 7.26 ppm or DMSO at 2.50 ppm. Electrospray ionization (ESI) mass spectra were recorded on an Acquity UPLC-Xevo G2 QT of mass spectrometer (Waters). Gel filtration chromatography was performed using a C18 column conjugated to an Agilent 1260 Infinite HPLC system. Prior to the characterization, each sample was purified via 0.45 μm filter to remove any aggregates. The flow rate was fixed at a rate of 0.5 mL/min, the injection volume was 10 μL and each sample was run for more than 15 min. Acetonitrile and water were used as the eluting solvent. UV/Vis absorption spectra were recorded on a PerkinElmer Lambda 465 UV-Vis spectrometer. Steady-state emission spectra were recorded on a Horiba FluoroMax-4 spectrofluorometer (Horiba Scientific). The light source (xenon lamp) that supplies UV excitation is focused onto the entrance slit of the excitation monochromator with an elliptical mirror. According to the manufacturer, the light source is a vertically mounted 150-W ozone-free cw xenon arc lamp. The distance between excitation and the sample is ~120 cm, and the integration time is 0.1 s. Fluorescence lifetime data were acquired with a 1 MHz LED laser with the excitation peak at 372 nm (NanoLED-370). Phosphorescence lifetime data were acquired with a 1 MHz LED laser with the excitation peak at 374 nm (SpectraLED-370). Lifetime data were analyzed with Data Station v6.6 (Horiba Scientific). Photographs were taken by a Canon EOS90D camera. The delayed emission spectra were recorded on Horiba FluoroMax-4 spectrofluorometer as well, using a 10-W xenon flash lamp as the excitation source with an integration time of 0.1 s. The absolute photoluminescence quantum yields were measured on a Horiba FluoroMax-4 spectrofluorometer (Horiba Scientific) with an integrating-sphere (Labsphere Inc.). Single crystal samples were obtained by slow evaporative crystallization of compounds in dichloromethane, chloroform or n-Hexane, and single crystal data was collected on a Bruker Smart APEXII CCD diffractometer using graphite monochromated Cu-Kα radiation (λ = 1.54178 Å). Podwer XRD was measured on Multifunctional Rotating-anode X-ray Diffractometer. Analytical thin layer chromatography (TLC) was performed using glass plates pre-coated with silica gel and zinc phosphate (0.25 mm). TLC plates were visualized by exposure to UV light at 254 nm. Flash column chromatography was performed using silica gel 60 (230-400 mesh) with the indicated solvents.

Sample Prepartion. All guest-host samples were prepared by serial dilution and subsequent evaporative drying form their dichloromethane (CH_2Cl_2) or $CHCl_3$ solutions. Specifically, a fixed amount of the host compound (100.00 mg) was place in a 5-mL vial, to which a dichloromethane solution of the guest with various concentrations and volumes was added. The liquid was vigorously mixed to yield a clear solution, which was then allowed to evaporate under the ambient condition for overnight. The crystalline solid was then collected and thoroughly dried in vacuum for at least 48 h prior to optical measurements. An example of the serial dilution of the guest molecule is provided: a stock solution (100 μl with a concentration

of 10.00 mg/mL) in dichloromethane was withdrawn and pipetted into a volumetric flask (10 mL), which yielded a dichloromethane solution with a concentration of 0.1 mg/mL. For each dilution, a concentration reduction by a factor of 100 can be achieved. And the exact mass of the guest molecule can be calculated by withdrawing from one of the four stock solutions (10.00, 0.1, 0.001, and 0.00001 mg/mL) in preparing the guest-host mixed solid samples. The pure host solid sample (control) was obtained by the same procedure by adding the same amount of dichloromethane without guest molecules to exclude any possibility of contaminant influence from solvents.

2. Supplementary Figures and Tables

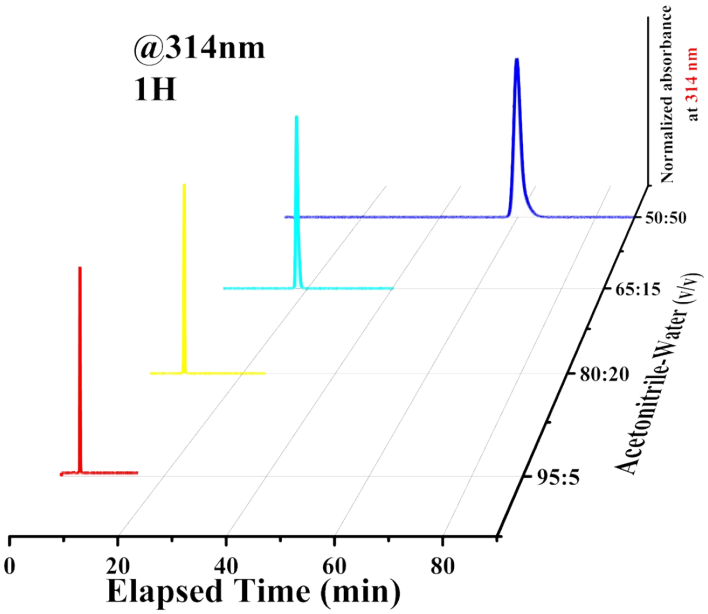

Figure S1. High performance liquid chromatogram (HPLC) spectrum of the model compound (**1H**) in acetonitrile (30 μM) with different proportions of acetonitrile and water monitored at the onset absorption of 314 nm.

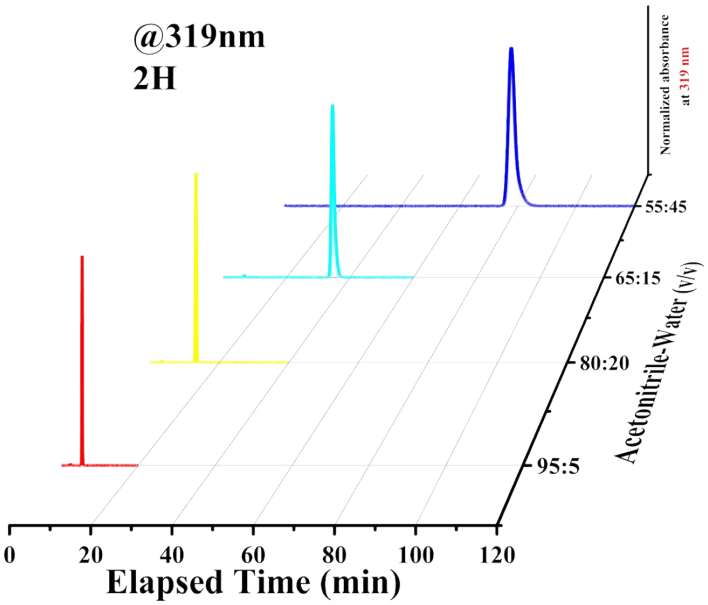

Figure S2. High performance liquid chromatogram (HPLC) spectrum of the model compound (**2H**) in acetonitrile (30 μM) with different proportions of acetonitrile and water monitored at the onset absorption of 319 nm.

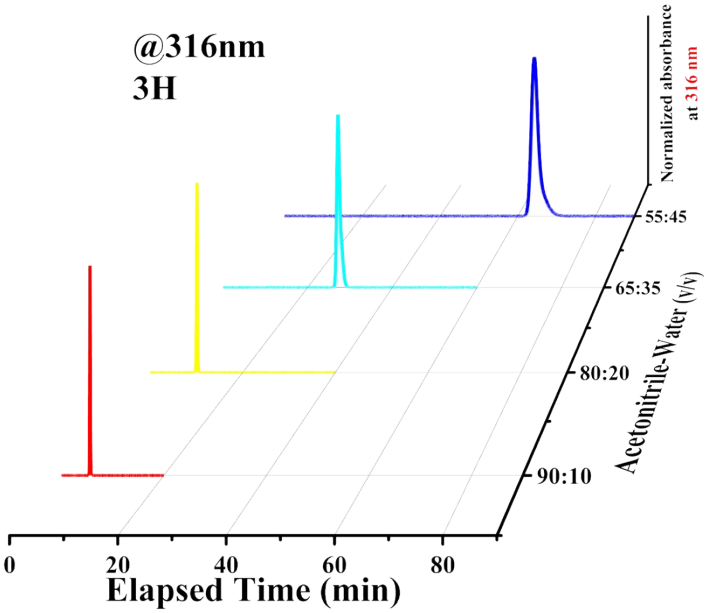

Figure S3. High performance liquid chromatogram (HPLC) spectrum of the model compound (**3H**) in acetonitrile (30 μM) with different proportions of acetonitrile and water monitored at the onset absorption of 316 nm .

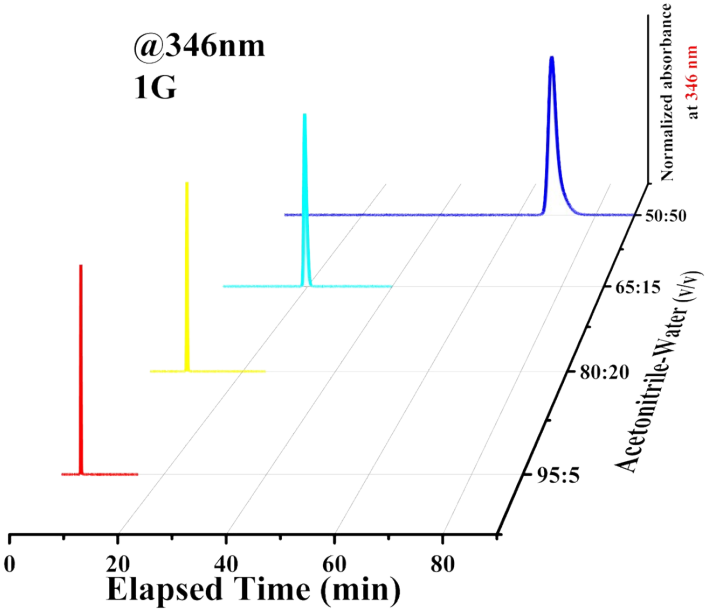

Figure S4. High performance liquid chromatogram (HPLC) spectrum of the model compound (**1G**) in acetonitrile (30 μM) with different proportions of acetonitrile and water monitored at the onset absorption of 346 nm.

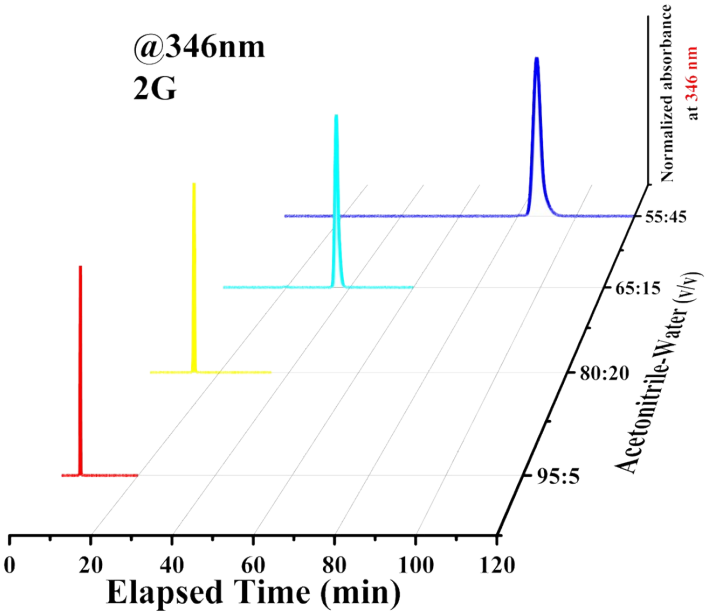

Figure S5. High performance liquid chromatogram (HPLC) spectrum of the model compound (**2G**) in acetonitrile (30 μM) with different proportions of acetonitrile and water monitored at the onset absorption of 346 nm.

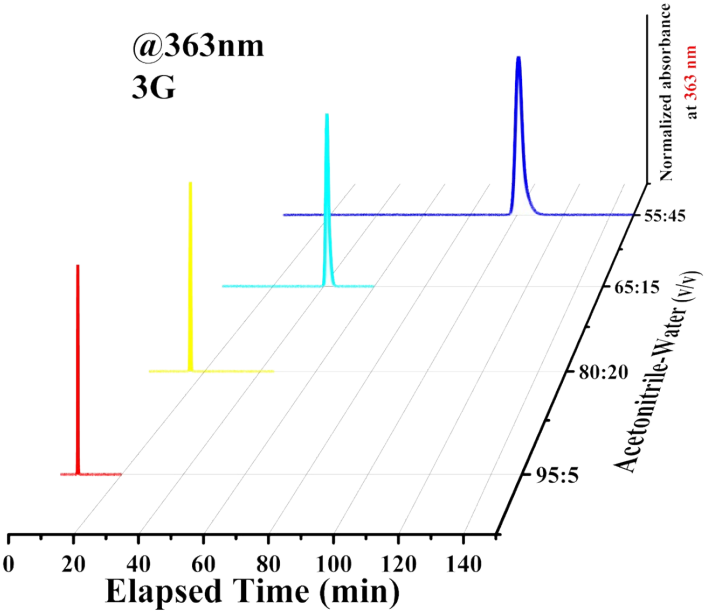

Figure S6. High performance liquid chromatogram (HPLC) spectrum of the model compound (**3G**) in acetonitrile (30 μM) with different proportions of acetonitrile and water monitored at the onset absorption of 363 nm.

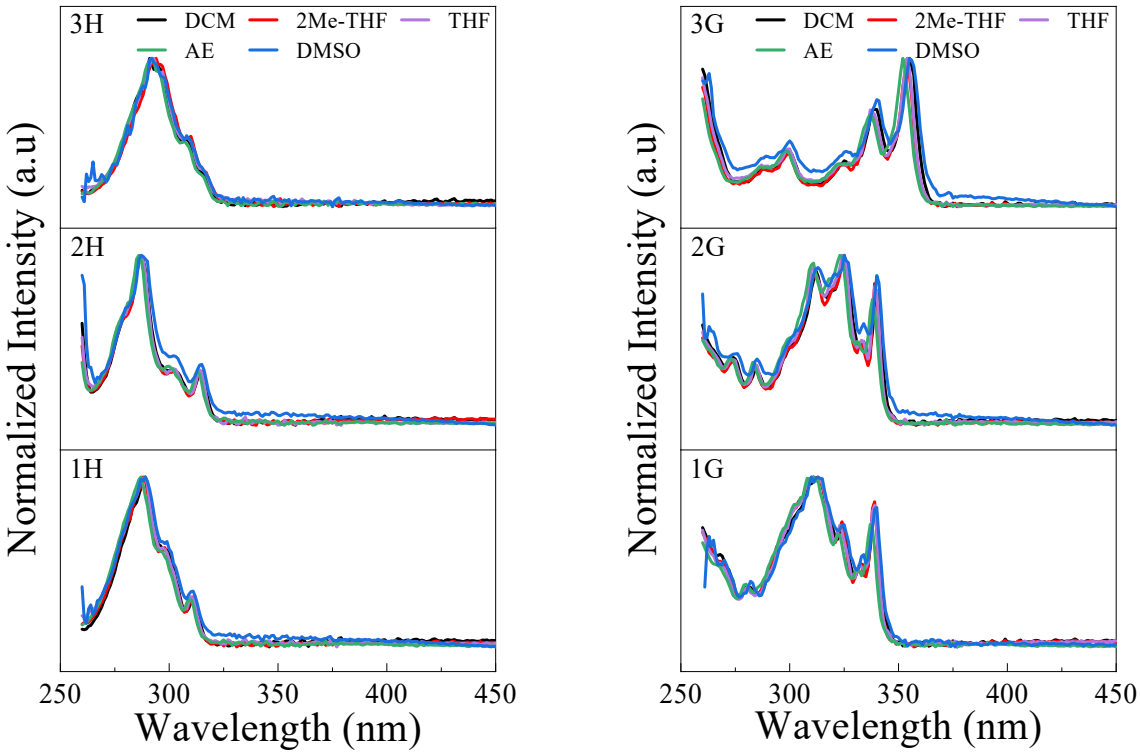

Figure S7. UV absorption spectra of model compound in different solvents (DCM: dichloromethane; 2-Me-THF 2-methyltetrahydrofuran; THF: tetrahydrofuran; AE: Acetonitrile; DMSO: Dimethyl sulfoxide; 0.25 mM) at 298 K.

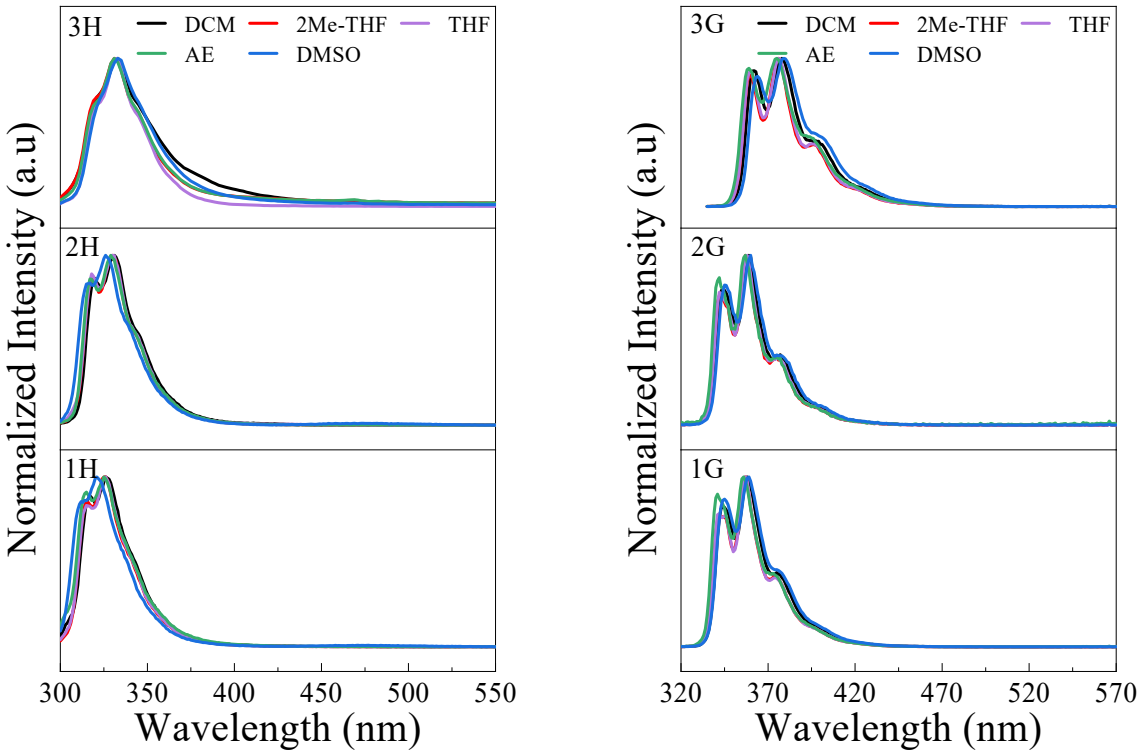

Figure S8. Photoluminescence (PL) spectra of model compound in different solvents (DCM: dichloromethane; 2-Me-THF: 2-methyltetrahydrofuran; THF: tetrahydrofuran; AE: Acetonitrile; DMSO: Dimethyl sulfoxide; 0.25 mM) at 298 K.

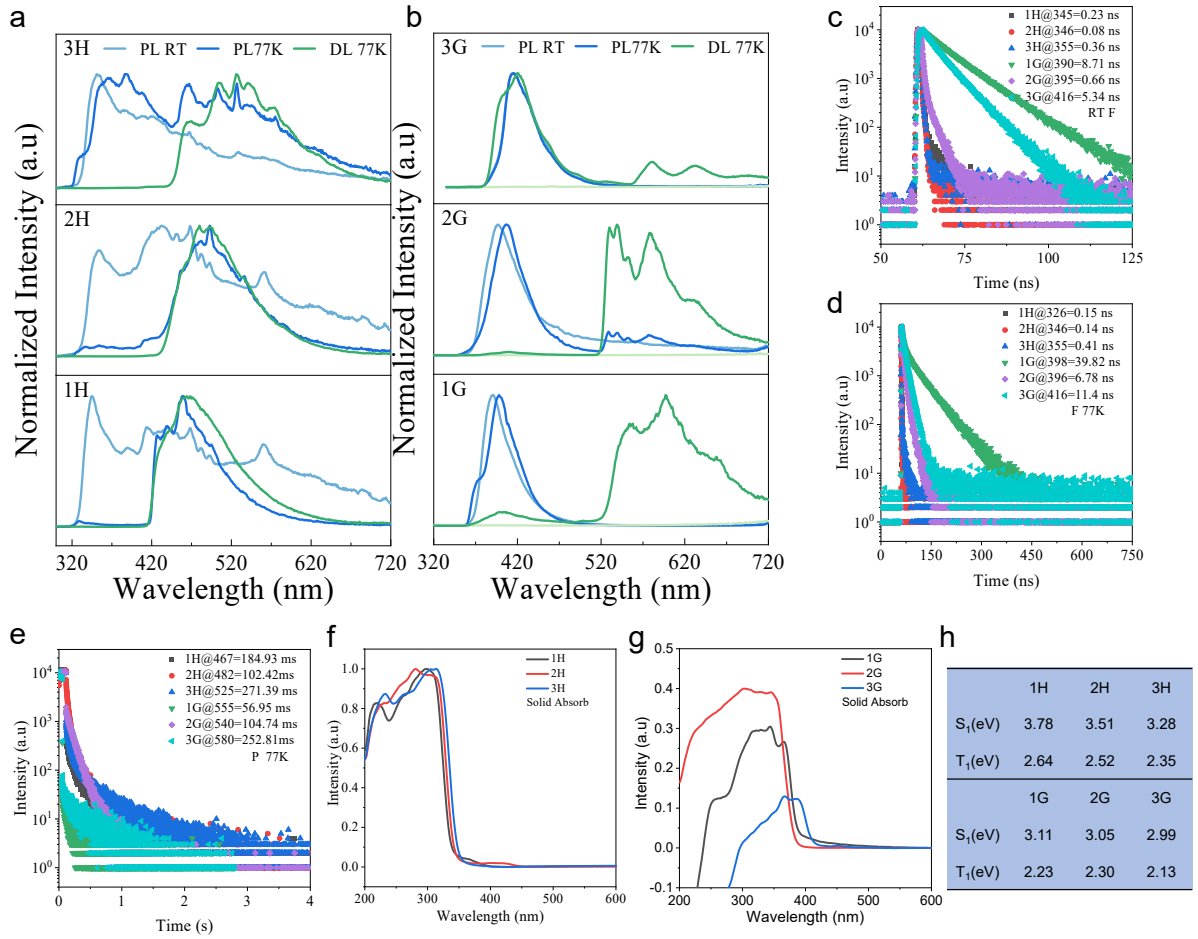

	1H	2H	3H
S_1(eV)	3.78	3.51	3.28
T_1(eV)	2.64	2.52	2.35
	1G	2G	3G
S_1(eV)	3.11	3.05	2.99
T_1(eV)	2.23	2.30	2.13

Figure S9. Steady-state photoluminescence emission (PL), delayed emission (DL) spectra ((a) and (b)) and emission decay curves ((c) fluorescence lifetime at 298 K; fluorescence lifetime (d) and phosphorescence lifetime (e) at 77 K) of the model compound in solid state. (f-g) UV-visible absorption spectra in solid state. (h) Calculated energy levels of the lowest excited single state (S1) and the lowest excited triplet state (T1) for dimer.

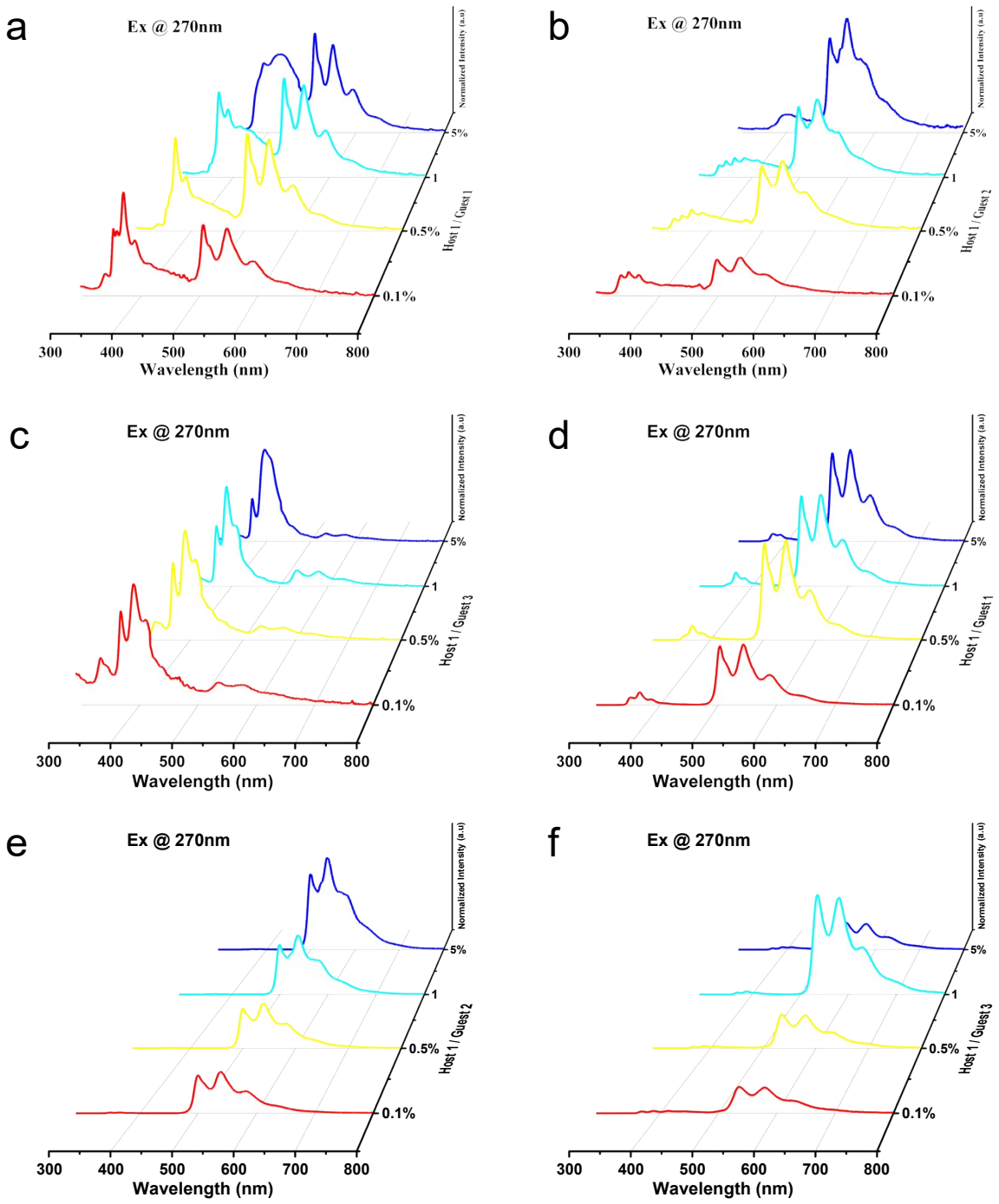

Figure S10. Steady-state photoluminescence emission (a-c) and delayed emission (d-f) spectra of three different guests (1G, 2G, and 3G) doping at host 1 (1H) with different doping concentration (0.1%-5%).

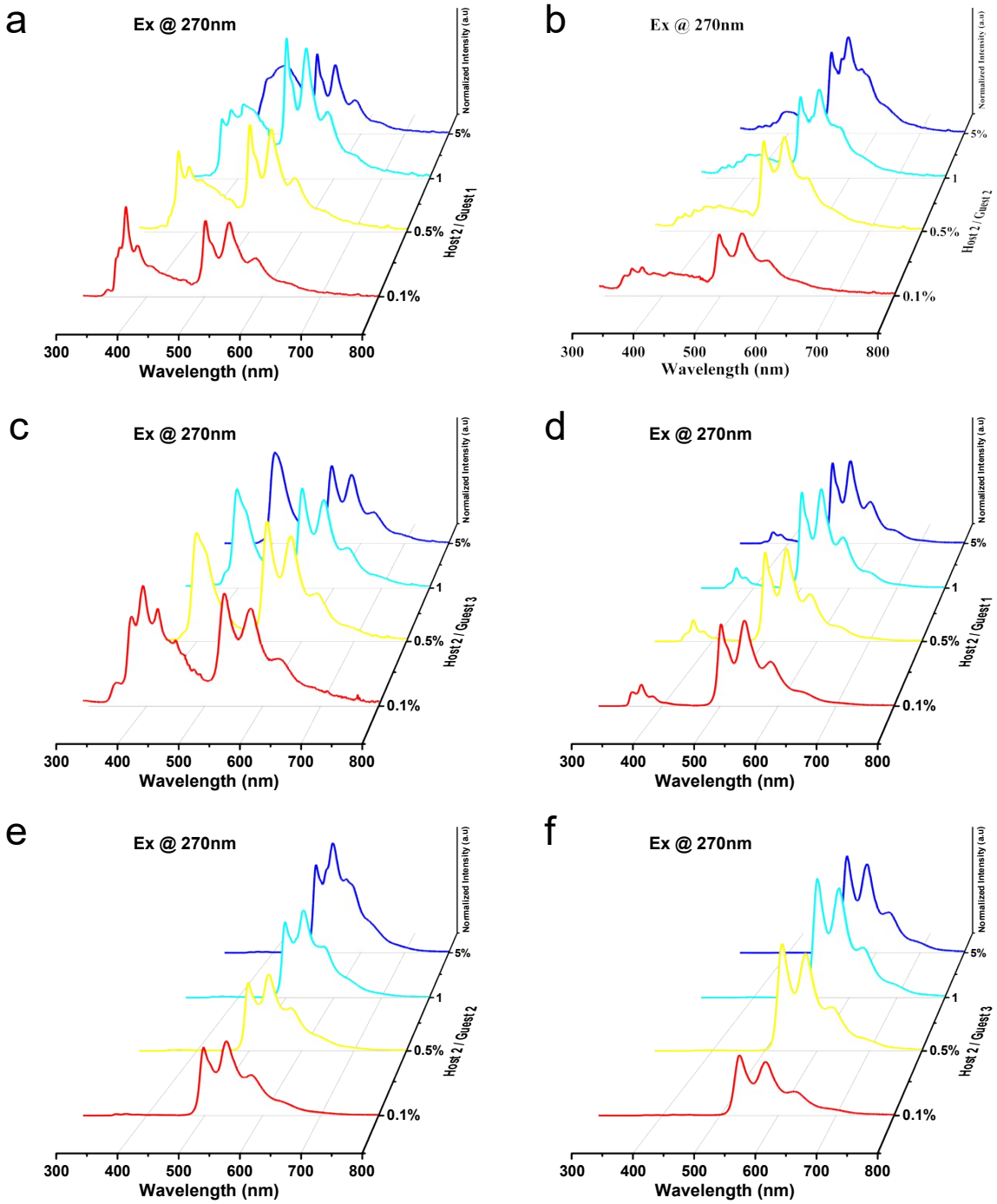

Figure S11. Steady-state photoluminescence emission (a-c) and delayed emission (d-f) spectra of three different guests (1G, 2G, and 3G) doping at host 2 (2H) with different doping concentration (0.1%-5%).

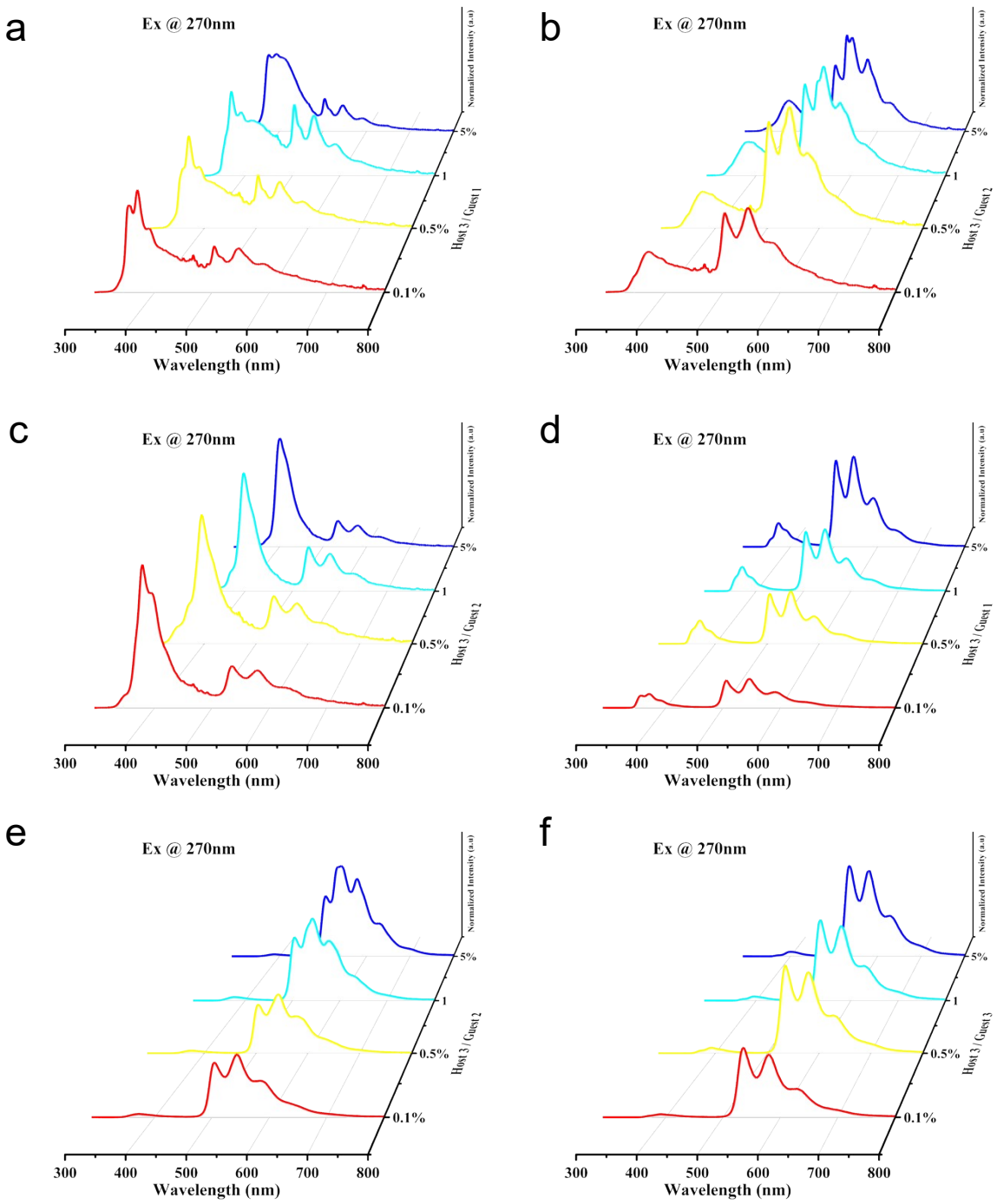

Figure S12. Steady-state photoluminescence emission (a-c) and delayed emission (d-f) spectra of three different guests (1G, 2G, and 3G) doping at host 3 (3H) with different doping concentration (0.1%-5%).

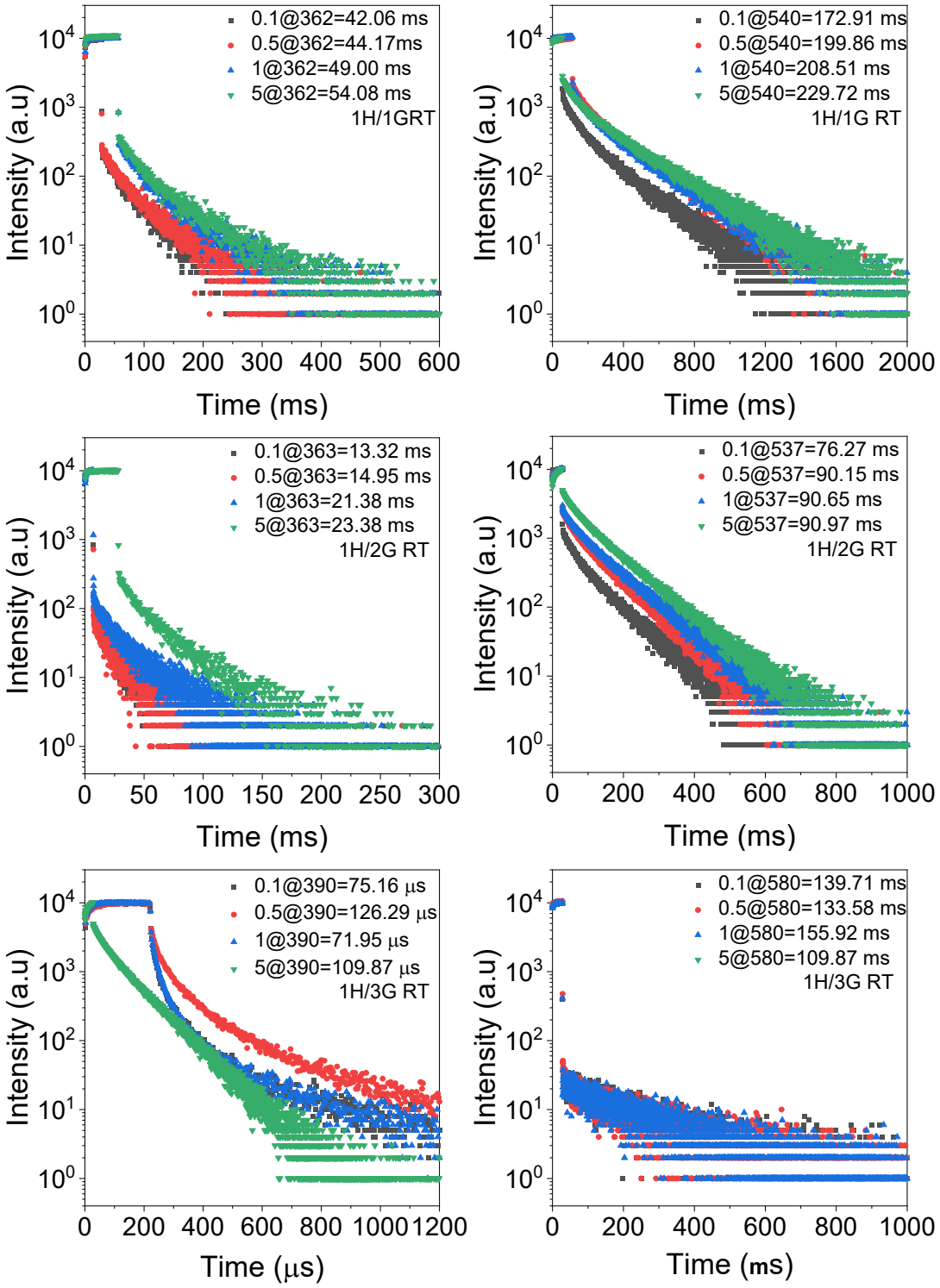

Figure S13. Time-resolved emission decay curves of three different guests (1G, 2G, and 3G) doping at host 1 (1H) with different doping concentration (0.1%-5%) at 298 K.

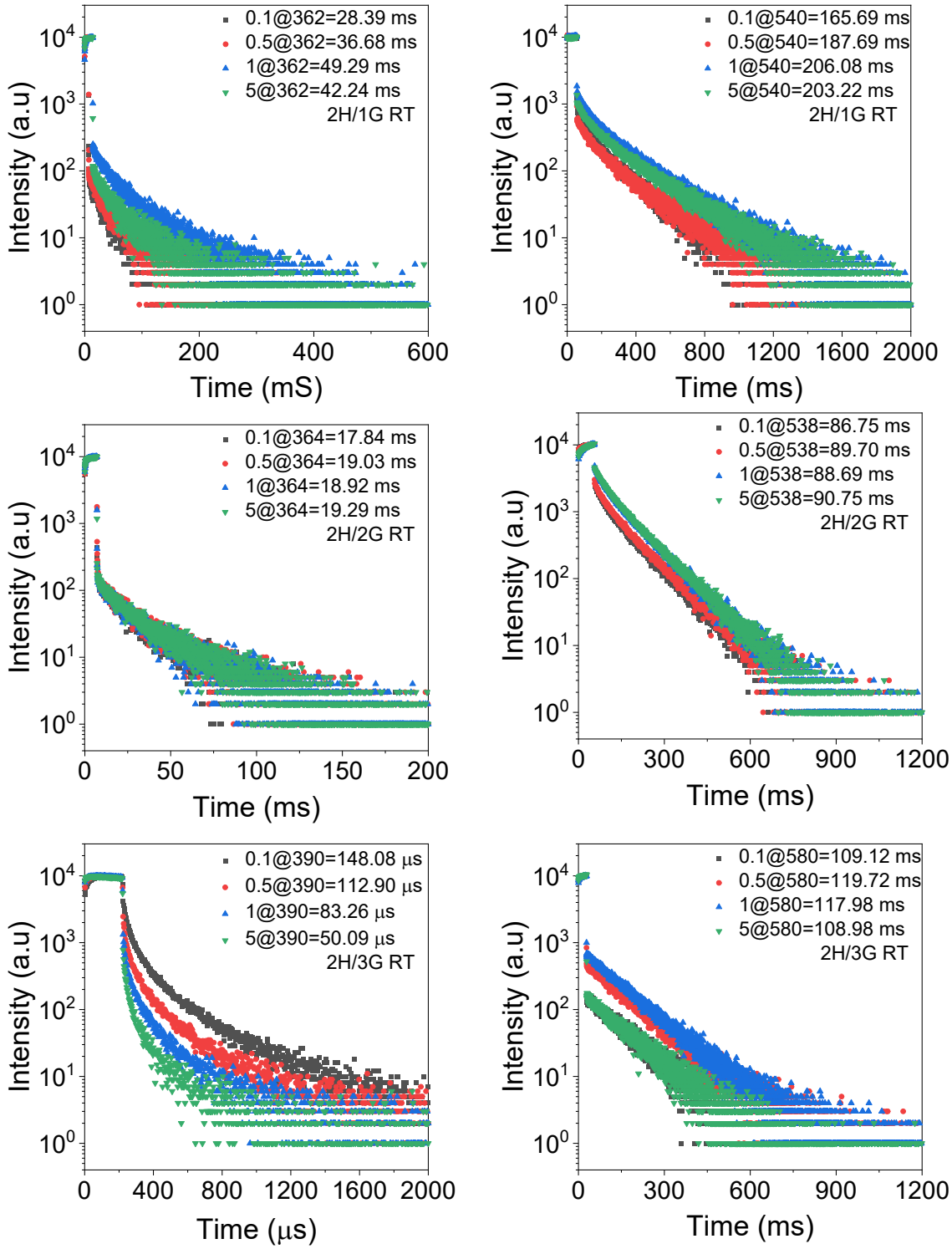

Figure S14. Time-resolved emission decay curves of three different guests (1G, 2G, and 3G) doping at host 2 (2H) with different doping concentration (0.1%-5%) at 298 K.

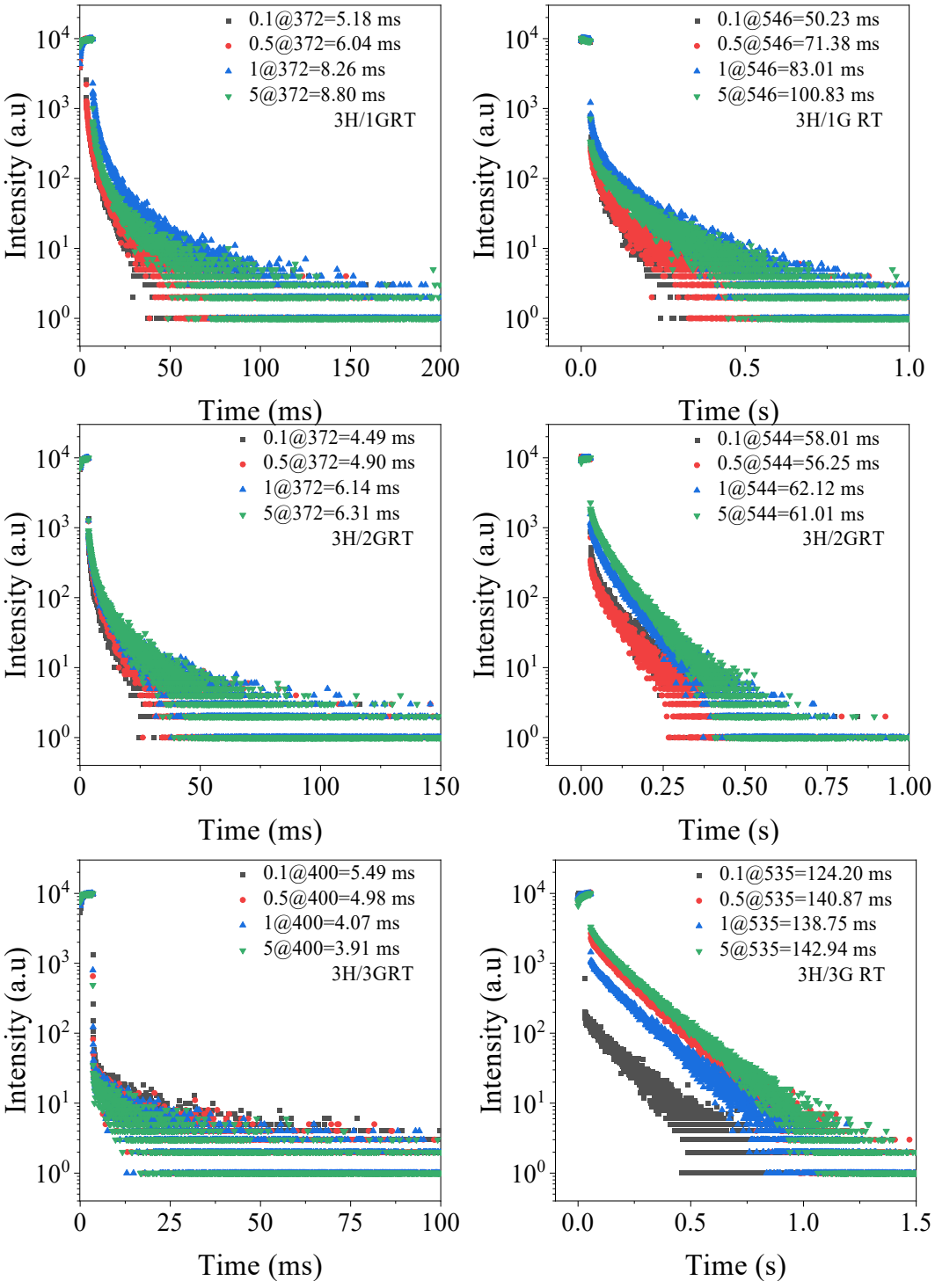

Figure S15. Time-resolved emission decay curves of three different guests (1G, 2G, and 3G) doping at host 3 (3H) with different doping concentration (0.1%-5%) at 298 K.

Table S1. Lifetimes summary of 1% dopant samples at room temperature from Fig. S13-15.

Guest\Host	1H	2H	3H
1G	49.00 ms@362 nm	49.29 ms@362 nm	8.26 ms@372 nm
2G	21.38 ms@363 nm	18.92 ms@364 nm	6.14 ms@372 nm
3G	71.95 μs@390 nm	83.26 μs@390 nm	4.07 ms@400 nm

Table S2. Lifetimes summary of 0.1% dopant samples at room temperature from Fig. S13-15.

Guest\Host	1H	2H	3H
1G	42.06 ms@362 nm	28.39 ms@362 nm	5.18 ms@372 nm
2G	13.32 ms@363 nm	17.84 ms@364 nm	4.49 ms@372 nm
3G	75.16 μs@390 nm	148.08 μs@390 nm	5.49 ms@400 nm

Table S3. Lifetimes summary of 0.5% dopant samples at room temperature from Fig. S13-15.

Guest\Host	1H	2H	3H
1G	44.17 ms@362 nm	36.68 ms@362 nm	6.04 ms@372 nm
2G	14.95 ms@363 nm	19.03 ms@364 nm	4.90 ms@372 nm
3G	126.29 μs@390 nm	112.90 μs@390 nm	4.98 ms@400 nm

Table S4. Lifetimes summary of 5% dopant samples at room temperature from Fig. S13-15.

Guest\Host	1H	2H	3H
1G	54.08 ms@362 nm	42.24 ms@362 nm	8.80 ms@372 nm
2G	23.38 ms@363 nm	19.29 ms@364 nm	6.31 ms@372 nm
3G	109.87 μs@390 nm	50.09 μs@390 nm	3.91 ms@400 nm

Table S5. Lifetimes summary of 1% dopant samples at room temperature from Fig. S13-15.

Guest\Host	1H	2H	3H
1G	208.51 ms@540 nm	206.08 ms@540 nm	83.01 ms@546 nm
2G	90.65 ms@537 nm	88.69 ms@538 nm	62.12 ms@544 nm
3G	155.92 ms@580 nm	117.98 ms@580 nm	138.75 ms@535 nm

Table **S6**. Lifetimes summary of 0.1% dopant samples at room temperature from Fig. S13-15.

Guest\Host	1H	2H	3H
1G	172.91 ms@540 nm	165.69 ms@540 nm	50.23 ms@546 nm
2G	76.27 ms@537 nm	86.75 ms@538 nm	58.01 ms@544 nm
3G	139.71 ms@580 nm	109.12 ms@580 nm	124.20 ms@535 nm

Table **S7**. Lifetimes summary of 0.5% dopant samples at room temperature from Fig. S13-15.

Guest\Host	1H	2H	3H
1G	199.86 ms@540 nm	187.69 ms@540 nm	71.38 ms@546 nm
2G	90.15 ms@537 nm	89.70 ms@538 nm	56.25 ms@544 nm
3G	133.58 ms@580 nm	119.72 ms@580 nm	140.87 ms@535 nm

Table **S8**. Lifetimes summary of 5% dopant samples at room temperature from Fig. S13-15.

Guest\Host	1H	2H	3H
1G	229.72 ms@540 nm	203.22 ms@540 nm	100.83 ms@546 nm
2G	90.97 ms@537 nm	90.75 ms@538 nm	61.01 ms@544 nm
3G	109.87 ms@580 nm	108.98 ms@580 nm	142.94 ms@535 nm

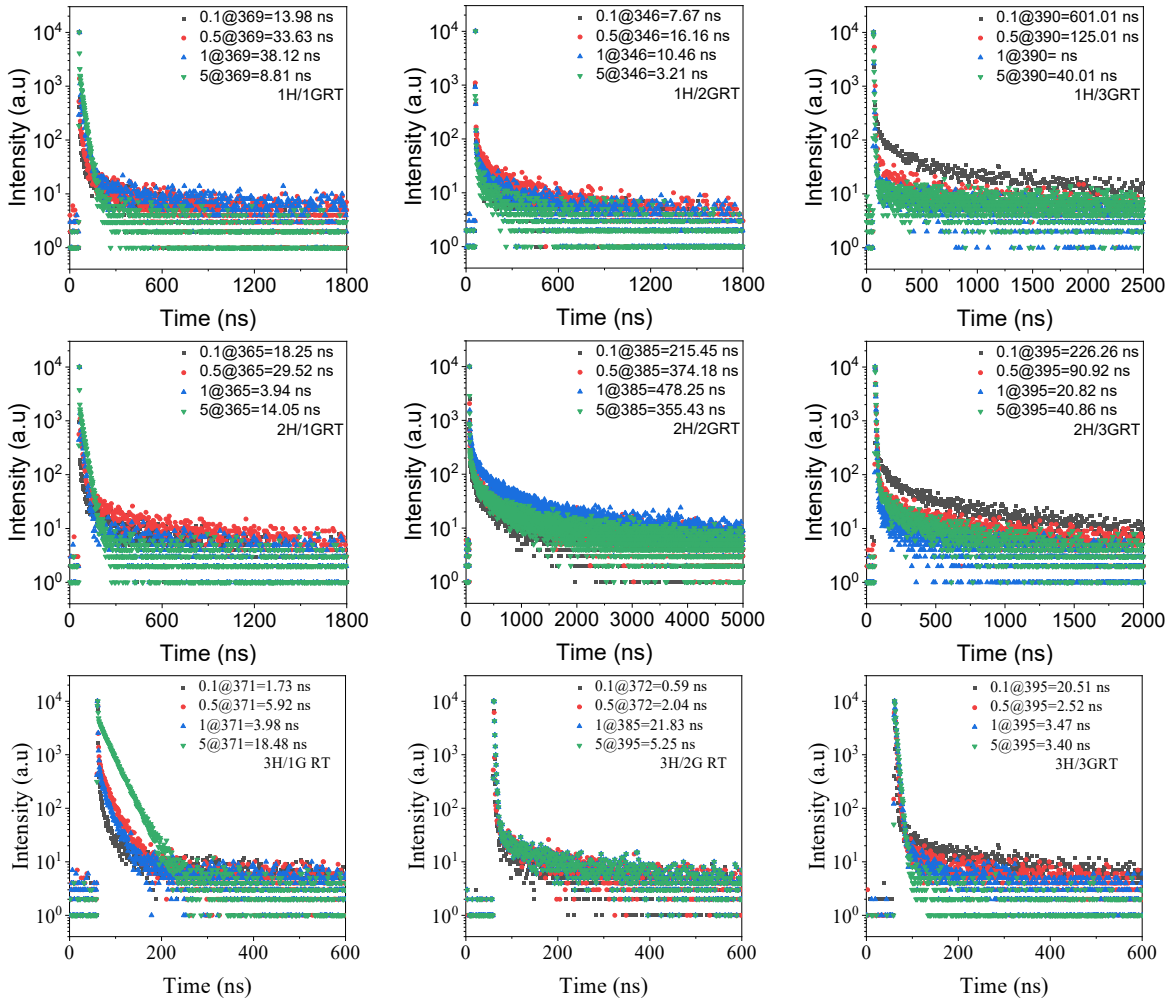

Figure S16. Time-resolved emission decay curves of three different guests (1G, 2G, and 3G) doping at three hosts with different doping concentration (0.1%-5%) at 298 K.

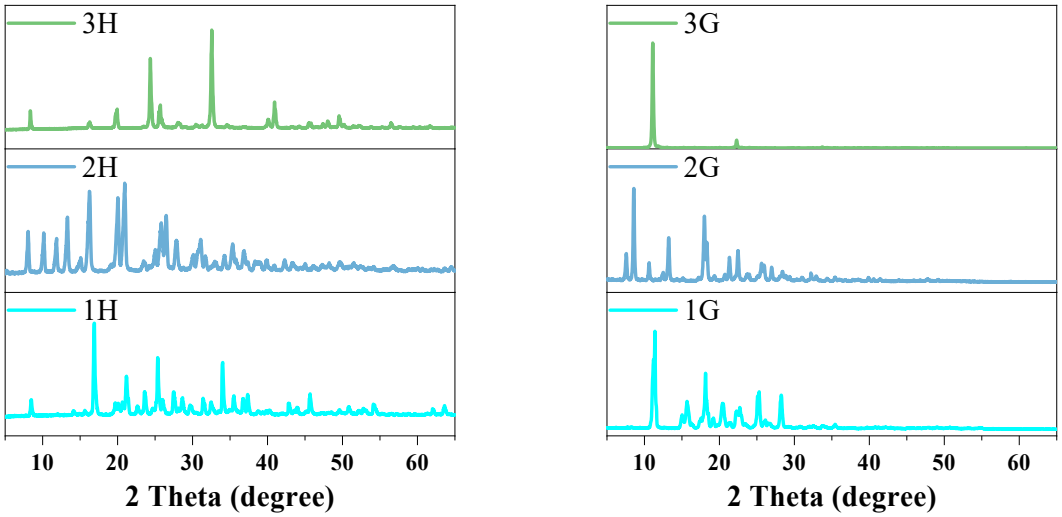

Figure S17. X-ray diffraction patterns of the pristine solid powders of pure host and guest.

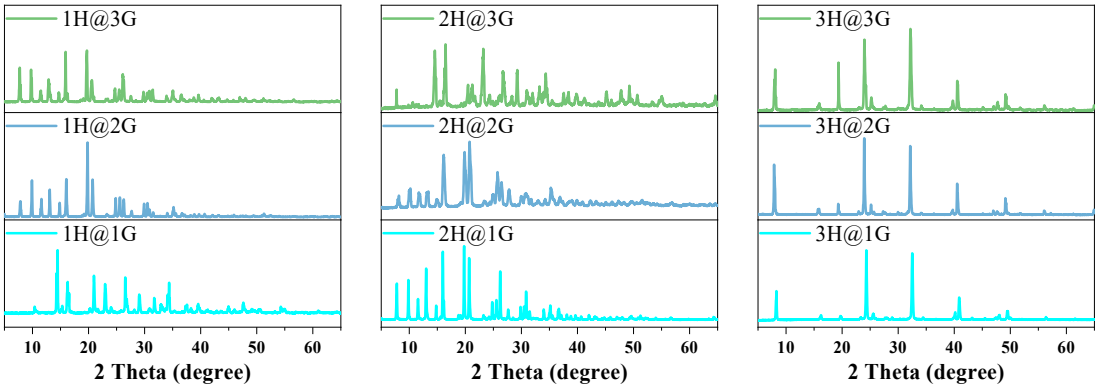

Figure S18. X-ray diffraction patterns of the host-guest doping samples (1% molar ratio).

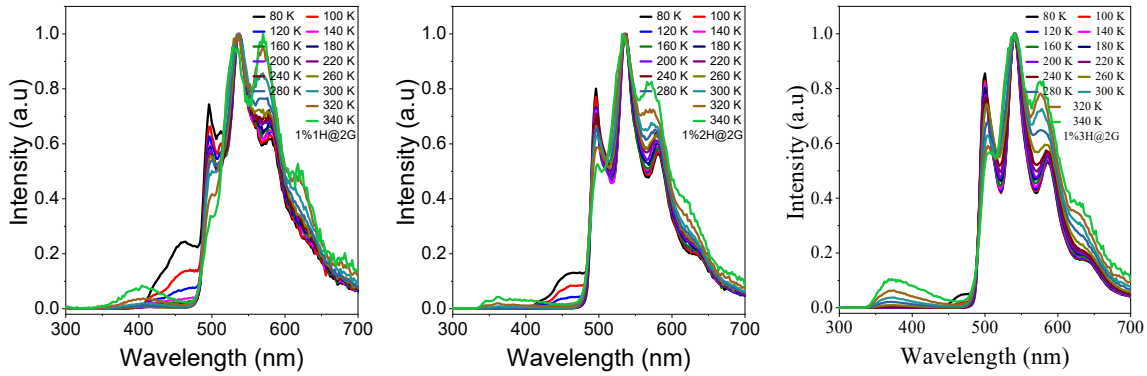

Figure S19. Temperature-dependent delayed emission (TDDE) spectra of the host-guest samples (2G-based samples), from 80 K to 340 K with 20 K interval.

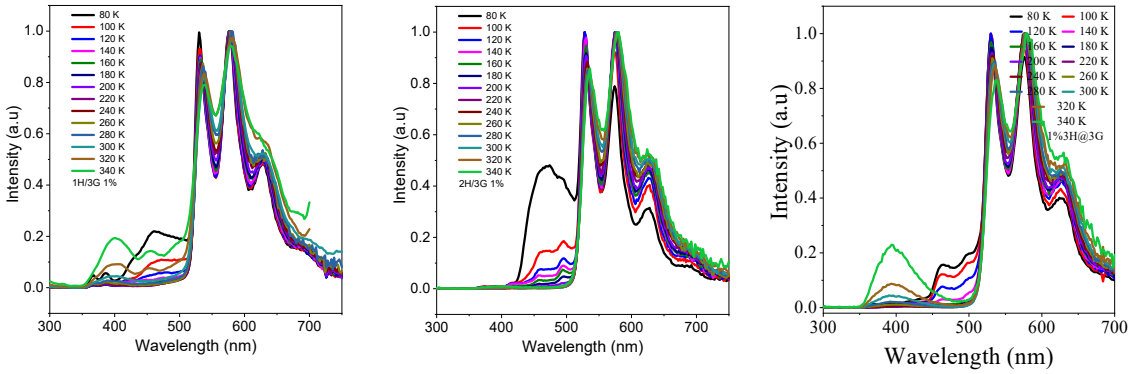

Figure S20. Temperature-dependent delayed emission (Δt = 0.1 ms, TDDE) spectra of ***S*-4FMNNI@*R*-4FBrBI** (10 ppm, λ_{ex} = 424 nm), from 79 K to 400 K with 10 K interval.

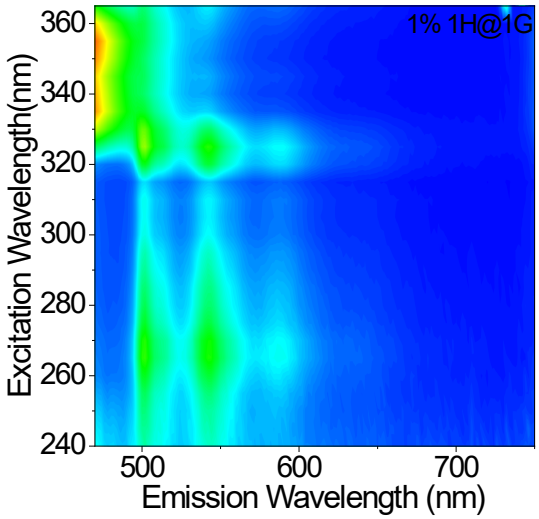

Figure S21. 2D Steady-state PL spectra of 1G dopants (1%) in 1H sample with different excitation wavelength from 240 nm to 360 nm.

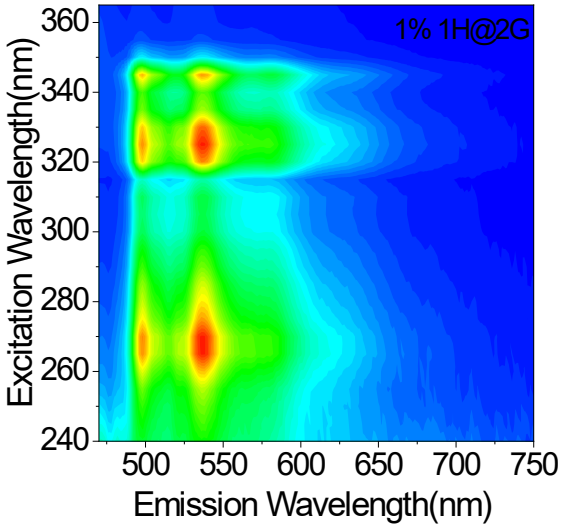

Figure S22. 2D Steady-state PL spectra of 2G dopants (1%) in 1H sample with different excitation wavelength from 240 nm to 360 nm.

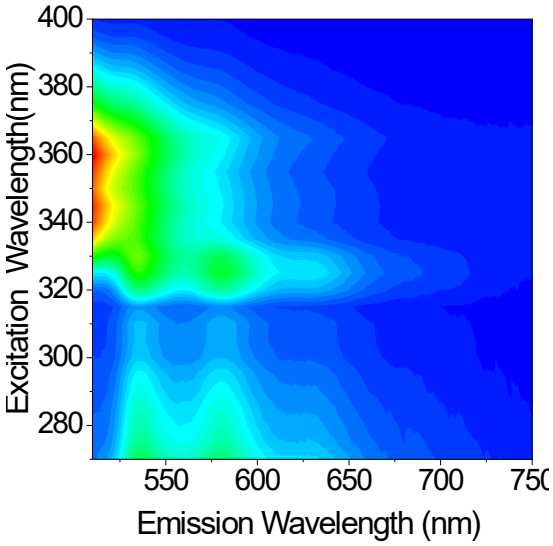

Figure S23. 2D Steady-state PL spectra of 3G dopants (1%) in 1H sample with different excitation wavelength from 240 nm to 360 nm.

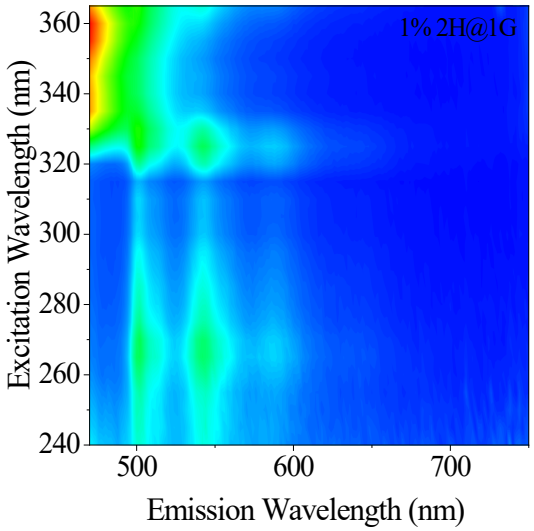

Figure S24. 2D Steady-state PL spectra of 1G dopants (1%) in 2H sample with different excitation wavelength from 240 nm to 360 nm.

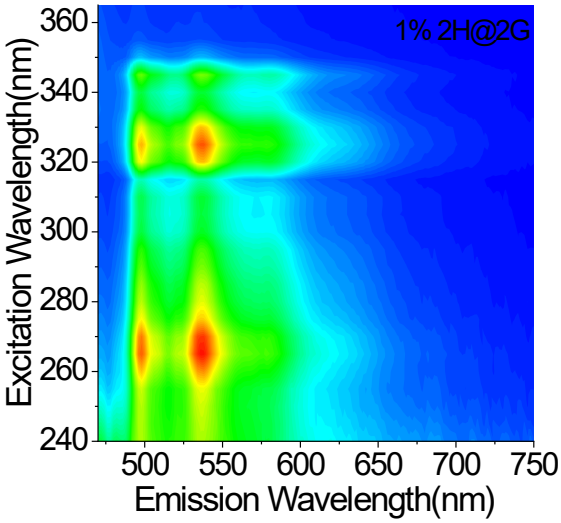

Figure S25. 2D Steady-state PL spectra of 2G dopants (1%) in 2H sample with different excitation wavelength from 240 nm to 360 nm.

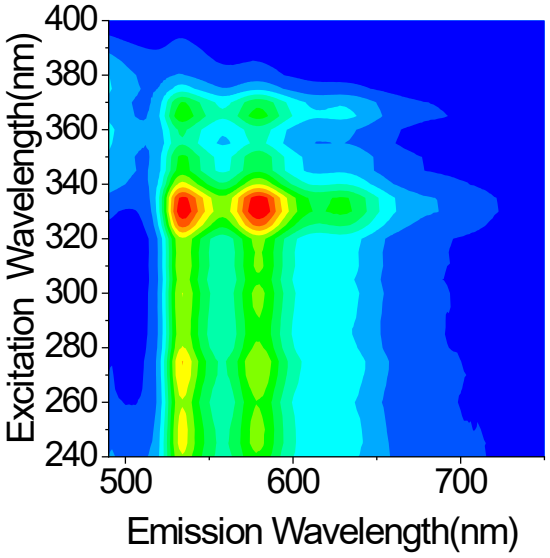

Figure S26. 2D Steady-state PL spectra of 3G dopants (1%) in 2H sample with different excitation wavelength from 240 nm to 360 nm.

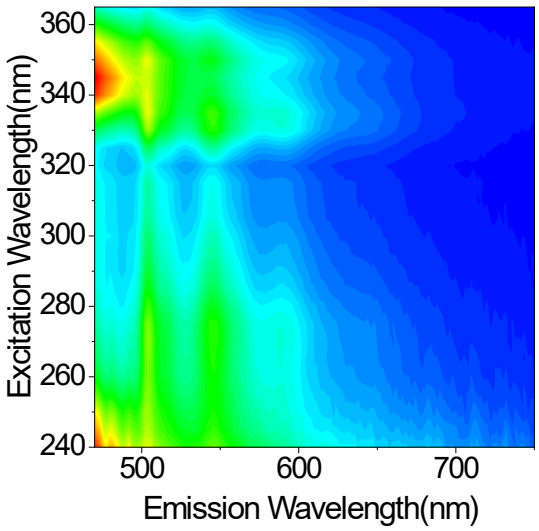

Figure S27. 2D Steady-state PL spectra of 1G dopants (1%) in 3H sample with different excitation wavelength from 240 nm to 360 nm.

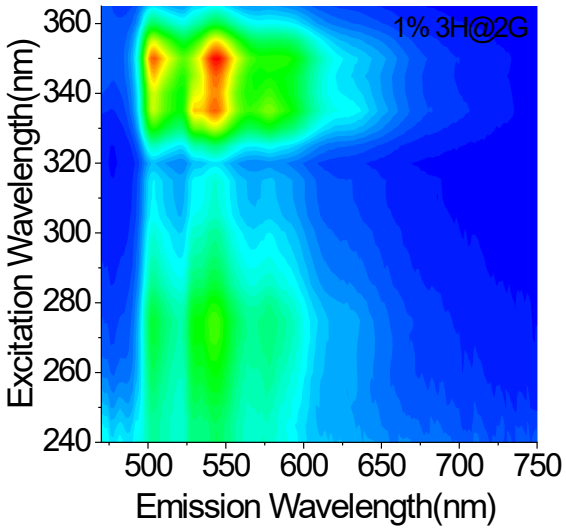

Figure S28. 2D Steady-state PL spectra of 2G dopants (1%) in 3H sample with different excitation wavelength from 240 nm to 360 nm.

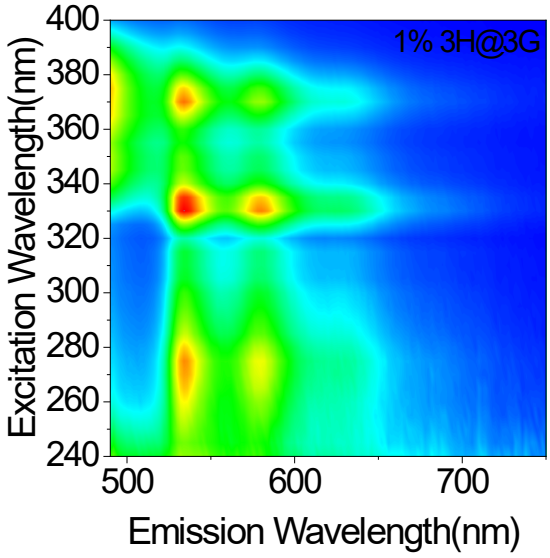

Figure S29. 2D Steady-state PL spectra of 3G dopants (1%) in 3H sample with different excitation wavelength from 240 nm to 360 nm.

3. Crystal data

Table S9. Crystal data and structure refinement for **1H** and **2H**.

Empirical formula	$C_{12}H_7BrO$	$C_{12}H_6BrClO$
	1H	**2H**
Formula weight	247.09	281.53
Temperature/K	293(2)	293(2)
Crystal system	monoclinic	monoclinic
Space group	$P2_1/c$	$P2_1/c$
a/Å	7.5889(11)	7.30216(14)
b/Å	5.9443(7)	11.5772(2)
c/Å	21.1757(19)	12.4218(3)
α/°	90	90
β/°	93.140(11)	97.5986(18)
γ/°	90	90
Volume/Å^3	953.8(2)	1040.89(4)
Z	4	4
ρ_{calc}g/cm^3	1.721	1.796
μ/mm^{-1}	4.267	7.465
F(000)	488.0	552.0
Crystal size/mm^3	0.21 × 0.2 × 0.18	0.2 × 0.2 × 0.2
Radiation	MoKα (λ = 0.71073)	CuKα (λ = 1.54184)
2Θ range for data collection/°	6.786 to 59.066	10.488 to 145.996
Index ranges	$-9 \leqslant h \leqslant 6$, $-8 \leqslant k \leqslant 7$, $-28 \leqslant l \leqslant 27$	$-8 \leqslant h \leqslant 4$, $-13 \leqslant k \leqslant 14$, $-15 \leqslant l \leqslant 15$
Reflections collected	5509	3876
Independent reflections	2272 [R_{int} = 0.0347, R_{sigma} = 0.0485]	2014 [R_{int} = 0.0148, R_{sigma} = 0.0152]
Data/restraints/parameters	2272/0/127	2014/0/136
Goodness-of-fit on F^2	1.054	1.073
Final R indexes [I>=2σ (I)]	R_1 = 0.0406, wR_2 = 0.072	R_1 = 0.0340, wR_2 = 0.0895
Final R indexes [all data]	R_1 = 0.0721, wR_2 = 0.0819	R_1 = 0.0360, wR_2 = 0.0912
Largest diff. peak/hole / e Å^{-3}	0.25/-0.39	0.44/-0.62

Table S10. Crystal data and structure refinement for **3H** and **2G**.

Empirical formula	C12H6BrClO	C16H9BrO
	3H	**2G**
Formula weight	281.53	297.14
Temperature/K	293.15	293(2)
Crystal system	orthorhombic	orthorhombic
Space group	$Pmn2_1$	$P2_12_12_1$
a/Å	22.2041(12)	3.98776(8)
b/Å	3.9193(2)	15.4203(3)
c/Å	5.8101(2)	19.0958(3)
α/°	90	90
β/°	90	90
γ/°	90	90
Volume/$Å^3$	505.62(4)	1174.25(4)
Z	2	4
$\rho_{calc}g/cm^3$	1.849	1.681
μ/mm^{-1}	7.684	4.615
F(000)	276.0	592.0
Crystal size/mm^3	0.13 × 0.12 × 0.1	0.2 × 0.2 × 0.2
Radiation	CuKα (λ = 1.54184)	CuKα (λ = 1.54184)
2Θ range for data collection/°	7.964 to 145.53	7.368 to 145.47
Index ranges	$-27 \leqslant h \leqslant 26$, $-4 \leqslant k \leqslant 3$, $-7 \leqslant l \leqslant 7$	$-4 \leqslant h \leqslant 3$, $-17 \leqslant k \leqslant 18$, $-23 \leqslant l \leqslant 22$
Reflections collected	2644	2661
Independent reflections	987 [R_{int} = 0.0785, R_{sigma} = 0.0569]	1868 [R_{int} = 0.0182, R_{sigma} = 0.0273]
Data/restraints/parameters	987/1/71	1868/0/163
Goodness-of-fit on F^2	1.103	1.083
Final R indexes [I>=2σ (I)]	R_1 = 0.0574, wR_2 = 0.1548	R_1 = 0.0256, wR_2 = 0.0656
Final R indexes [all data]	R_1 = 0.0575, wR_2 = 0.1549	R_1 = 0.0264, wR_2 = 0.0663
Largest diff. peak/hole / e $Å^{-3}$	1.28/-0.70	0.25/-0.55
Flack parameter	-0.01(9)	-0.009(17)

Table S11. Crystal data and structure refinement for **3G**.

Empirical formula	$C_{20}H_{12}O$
	3G
Formula weight	268.30
Temperature/K	170(2)
Crystal system	triclinic
Space group	P-1
a/Å	9.1041(12)
b/Å	13.9612(18)
c/Å	31.889(4)
α/°	91.084(5)
β/°	93.736(4)
γ/°	98.685(4)
Volume/Å^3	3996.6(9)
Z	12
ρ_{calc}g/cm^3	1.338
μ/mm^{-1}	
F(000)	1680
Crystal size/mm^3	0.34 × 0.18 × 0.16
Radiation	MoKα (λ = 0.71073)
2Θ range for data collection/°	2.27 to 26.42
Index ranges	-11 ⩽ h ⩽ 11, -17 ⩽ k ⩽ 17, -40 ⩽ l ⩽ 39
Reflections collected	9980
Independent reflections	16961 [R_{int} = 0.1432, R_{sigma} = 0.071]
Data/restraints/parameters	16961/0/1136
Goodness-of-fit on F^2	1.032
Final R indexes [I>=2σ (I)]	R_1 = 0.0947, wR_2 = 0.2659
Final R indexes [all data]	R_1 = 0.1566, wR_2 = 0.3210
Largest diff. peak/hole / e Å^{-3}	0.524/-0.340

4. Nuclear Magnetic Resonance (NMR) and High-Resolution Mass (HRM) Spectra

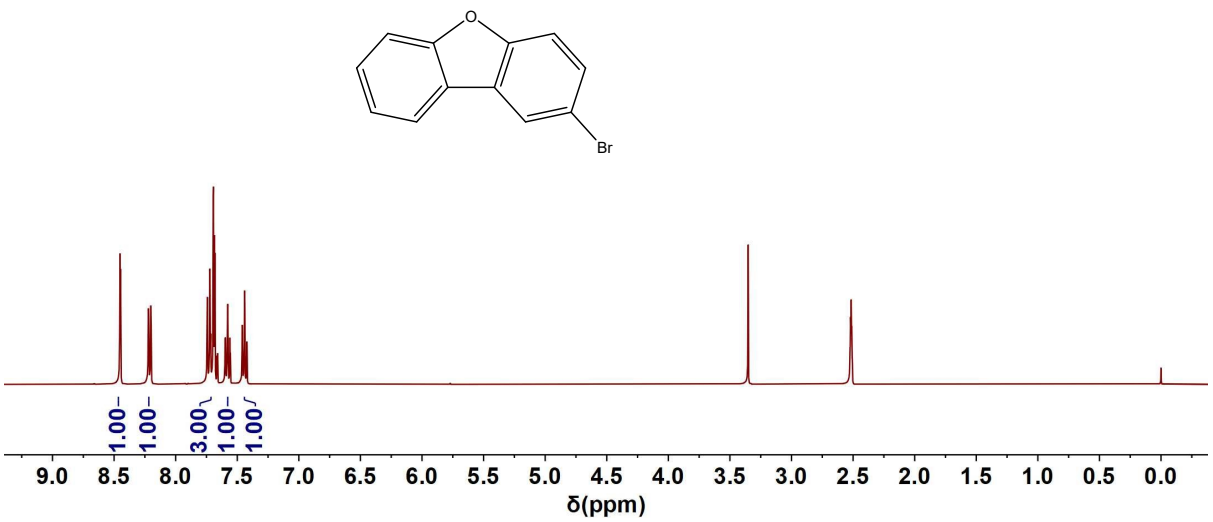

Figure S30. ^{1}H NMR spectrum of 1H in d-DMSO.

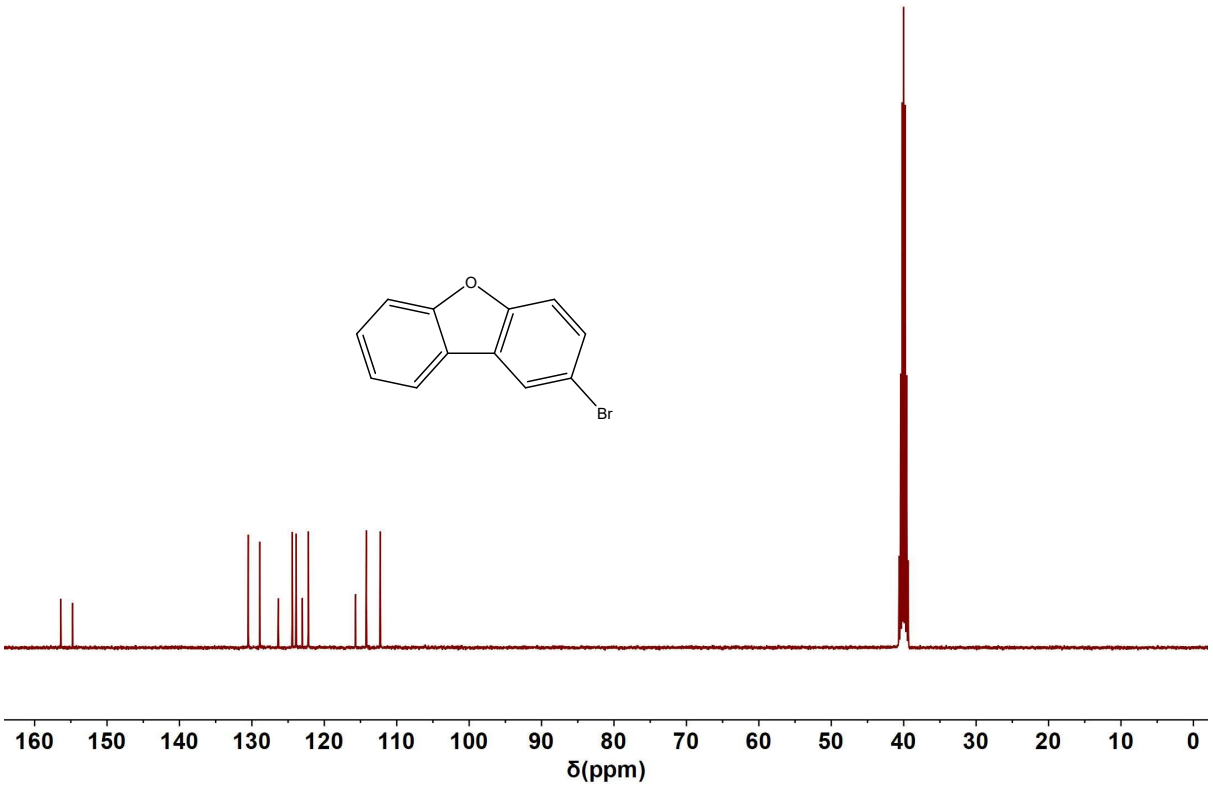

Figure S31. ^{13}C NMR spectrum of 1H in d-DMSO.

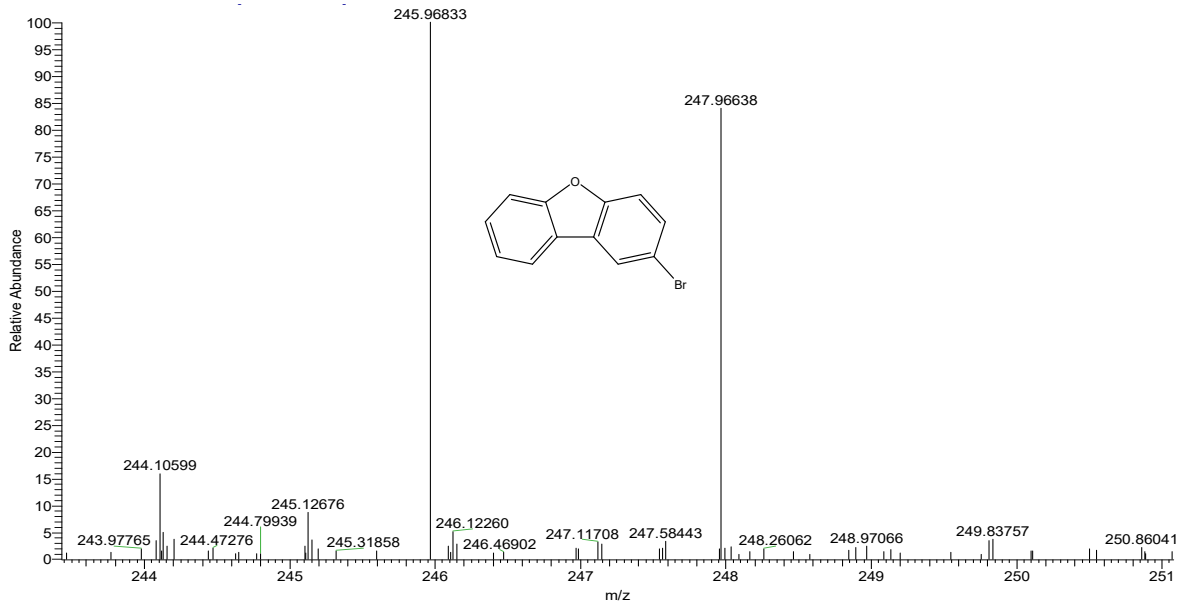

Figure S32. EI mass spectrum of 1H.

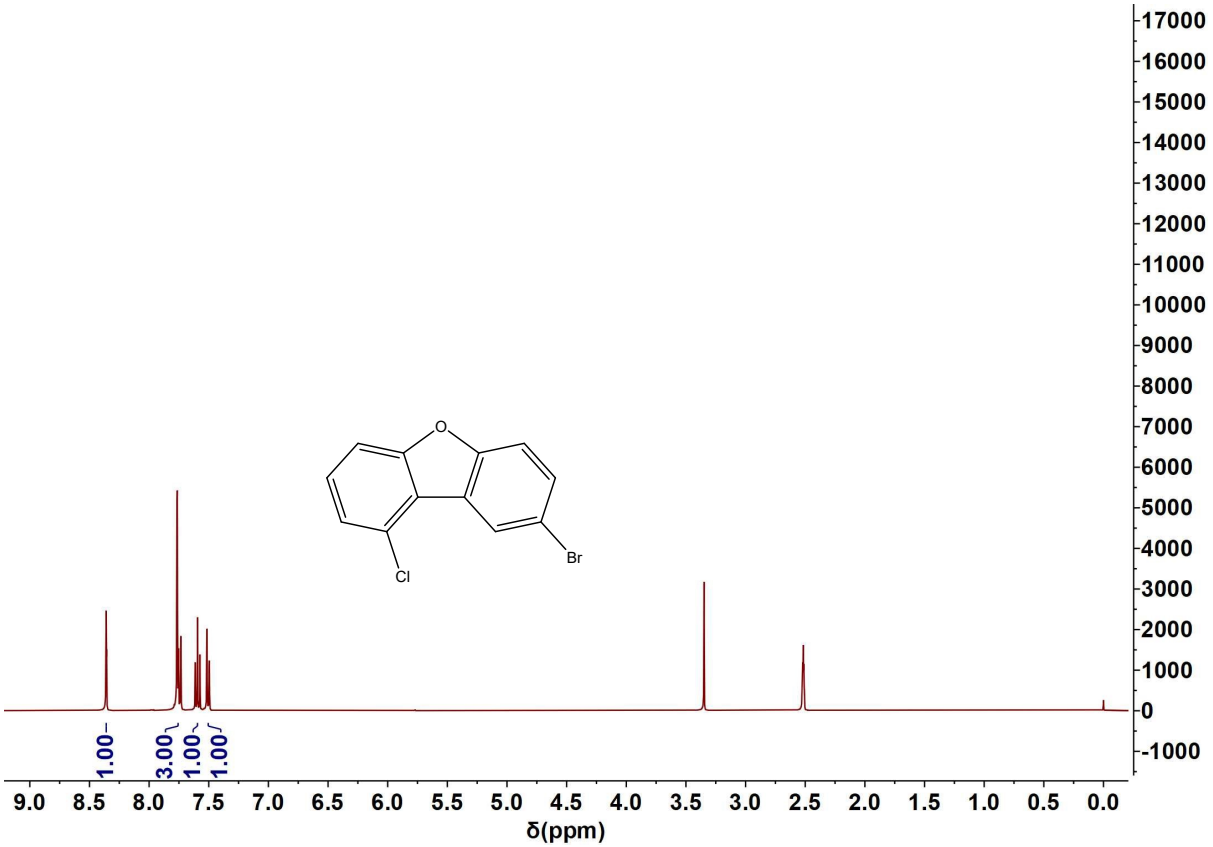

Figure S33. ^{1}H NMR spectrum of 2H in d-DMSO.

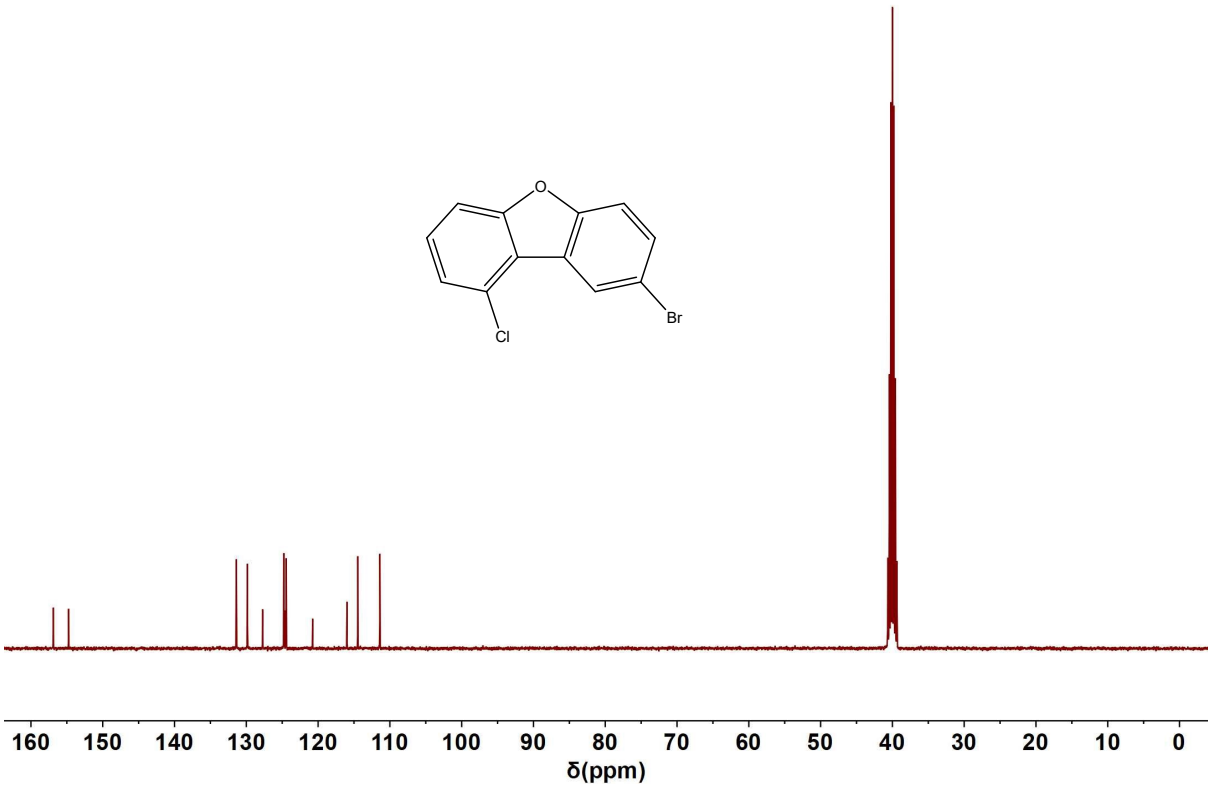

Figure S34. ^{13}C NMR spectrum of 2H in d-DMSO.

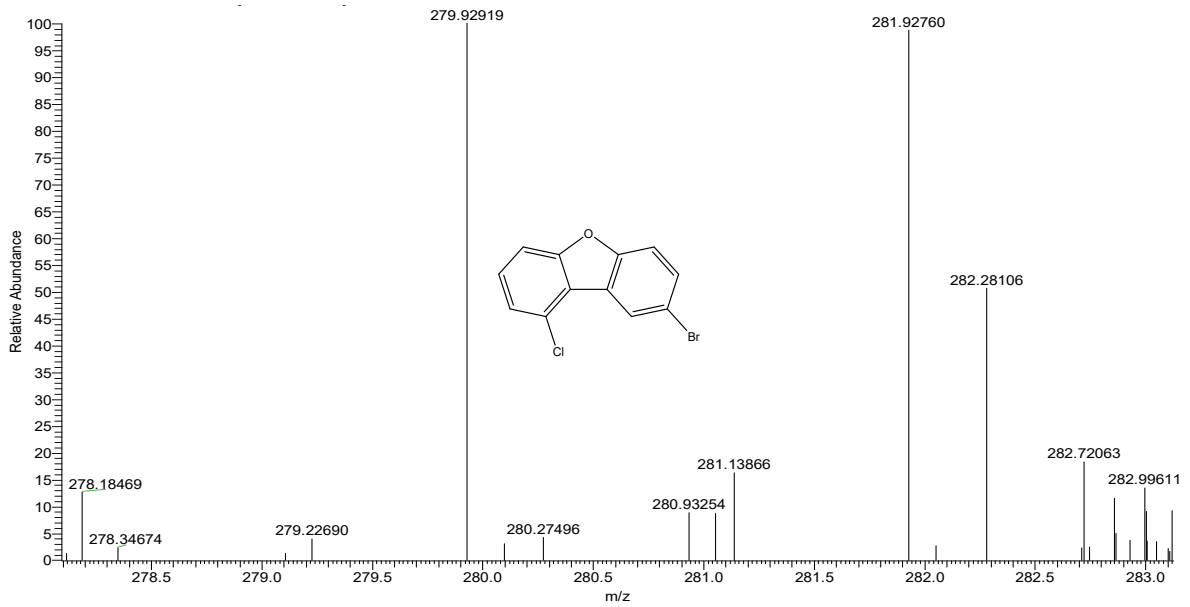

Figure S35. EI mass spectrum of 2H.

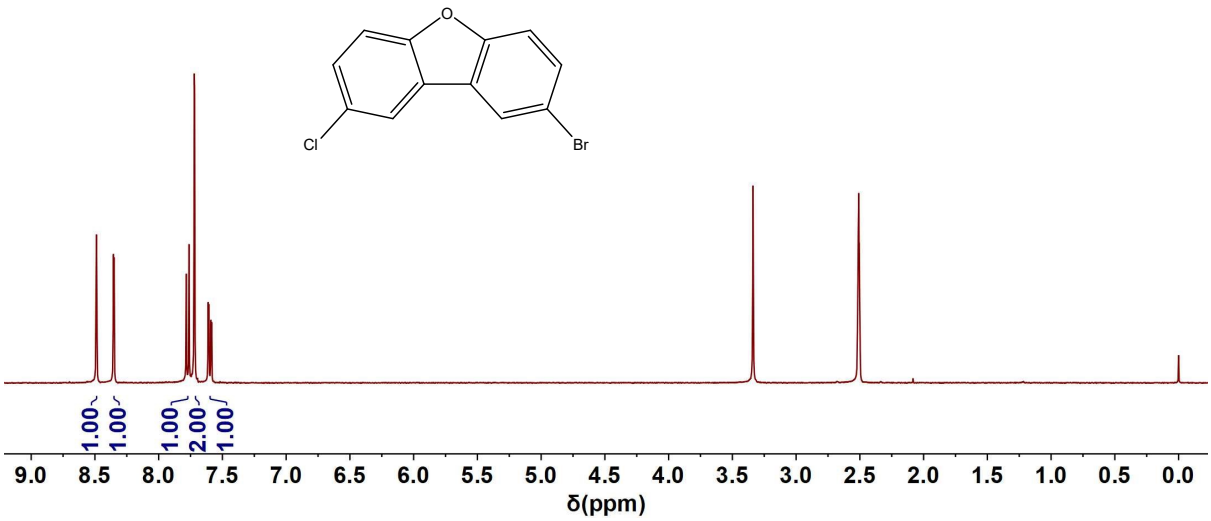

Figure S36. ^{1}H NMR spectrum of 3H in d-DMSO.

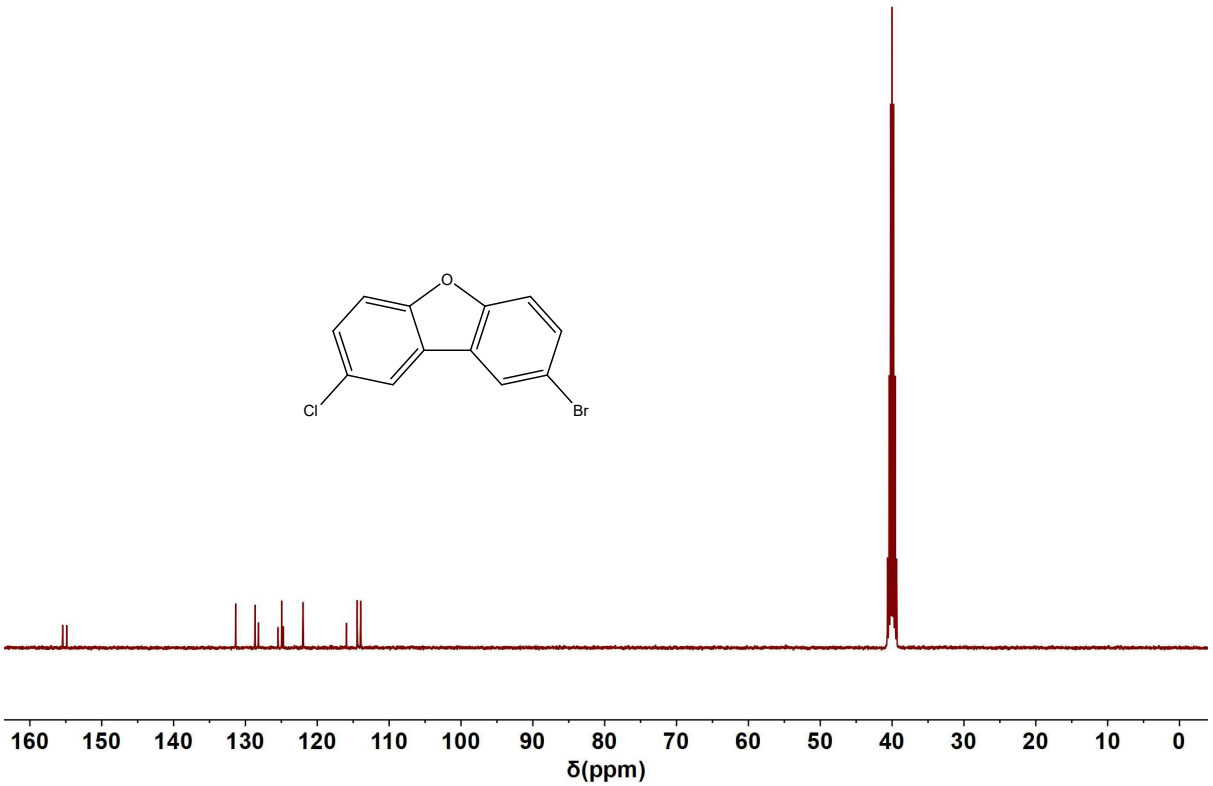

Figure S37. ^{13}C NMR spectrum of 3H in d-DMSO.

Figure S38. EI mass spectrum of 3H.

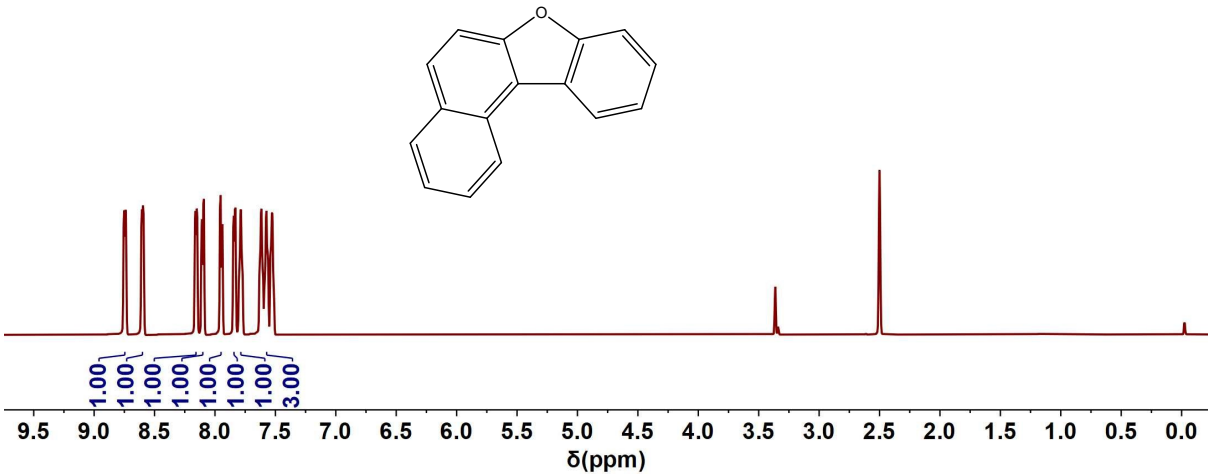

Figure S39. ^{1}H NMR spectrum of 1G in d-DMSO.

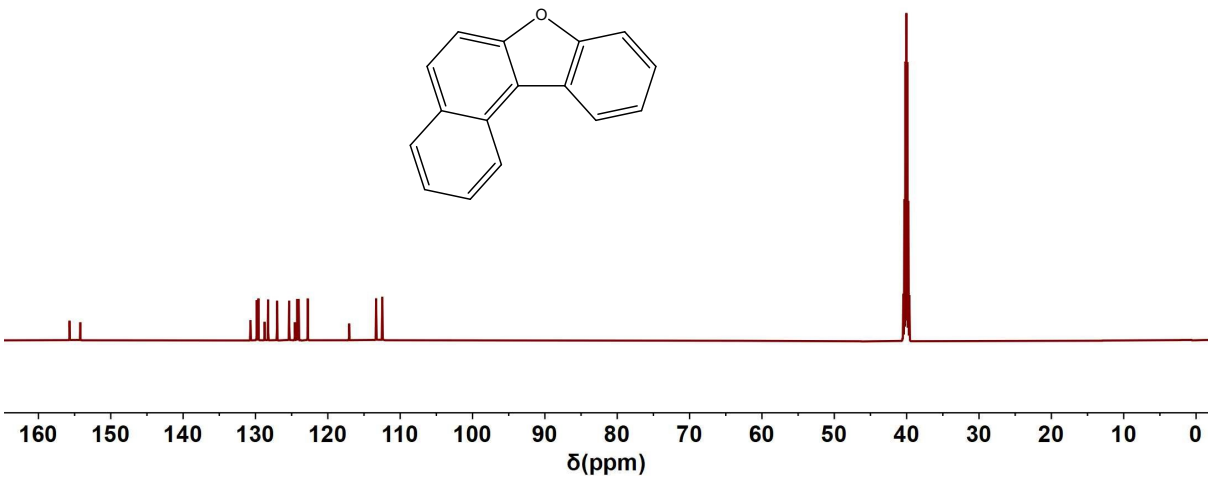

Figure S40. ^{13}C NMR spectrum of 1G **I** in d-DMSO.

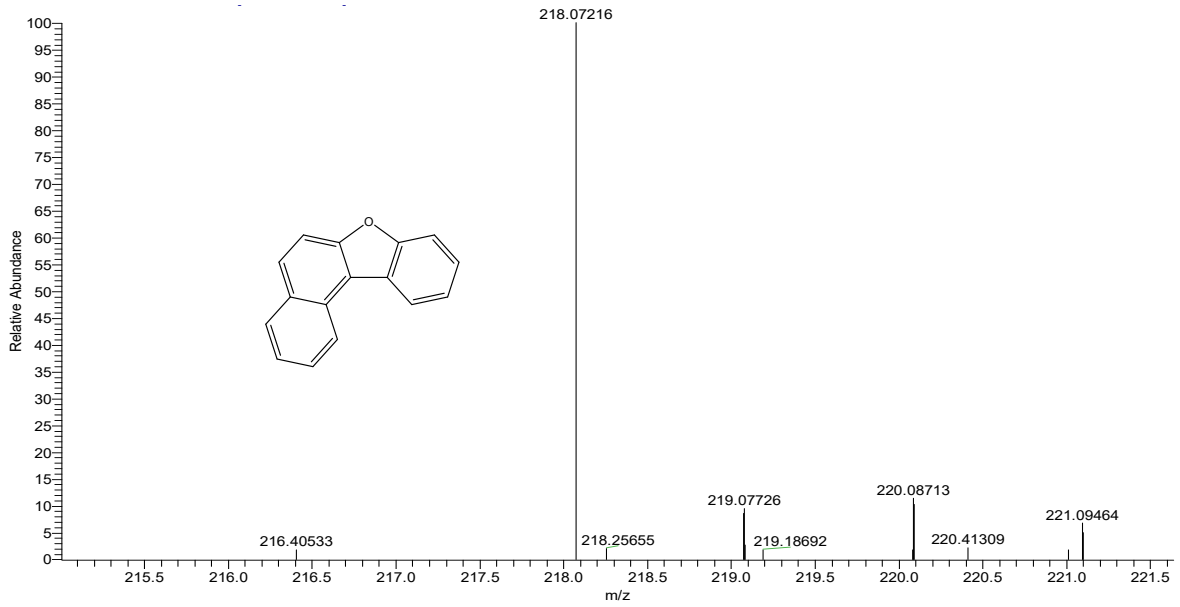

Figure S41. ESI mass spectrum of 1G.

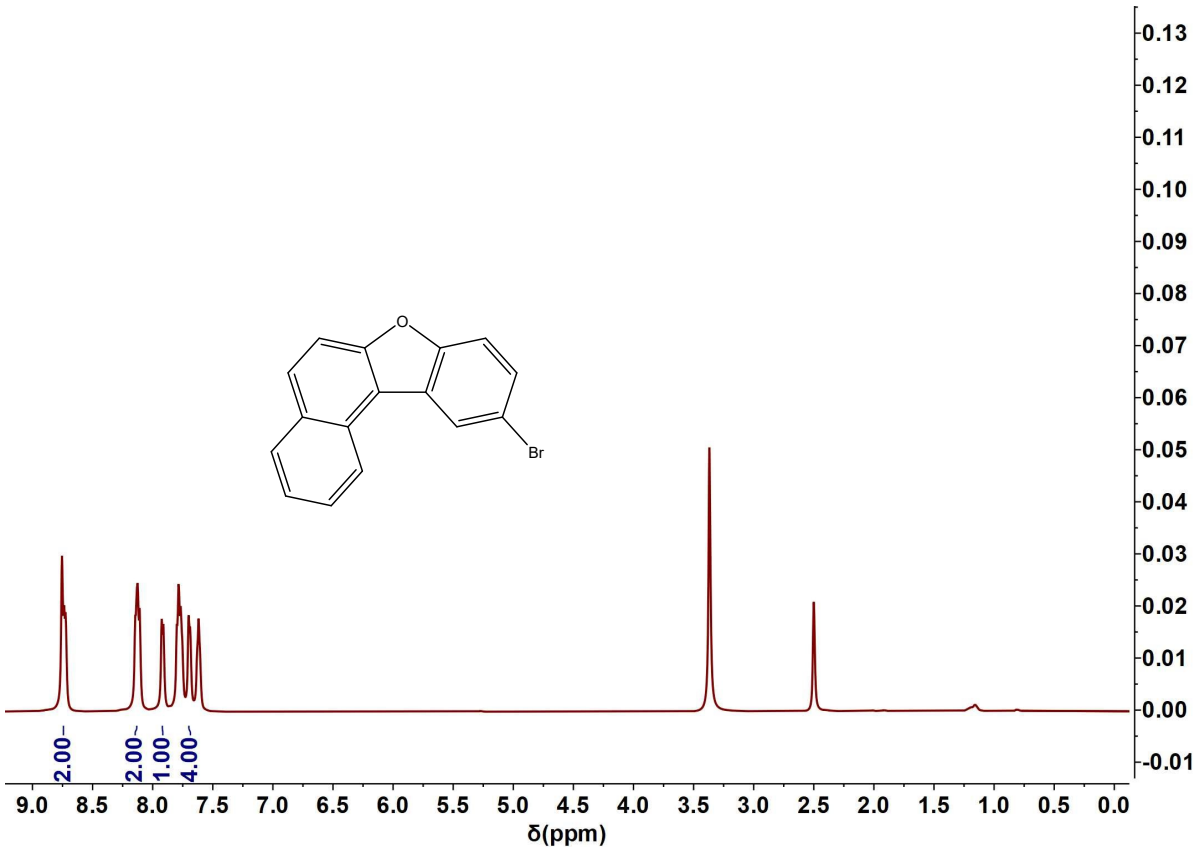

Figure S42. ^{1}H NMR spectrum of 2G in d-DMSO.

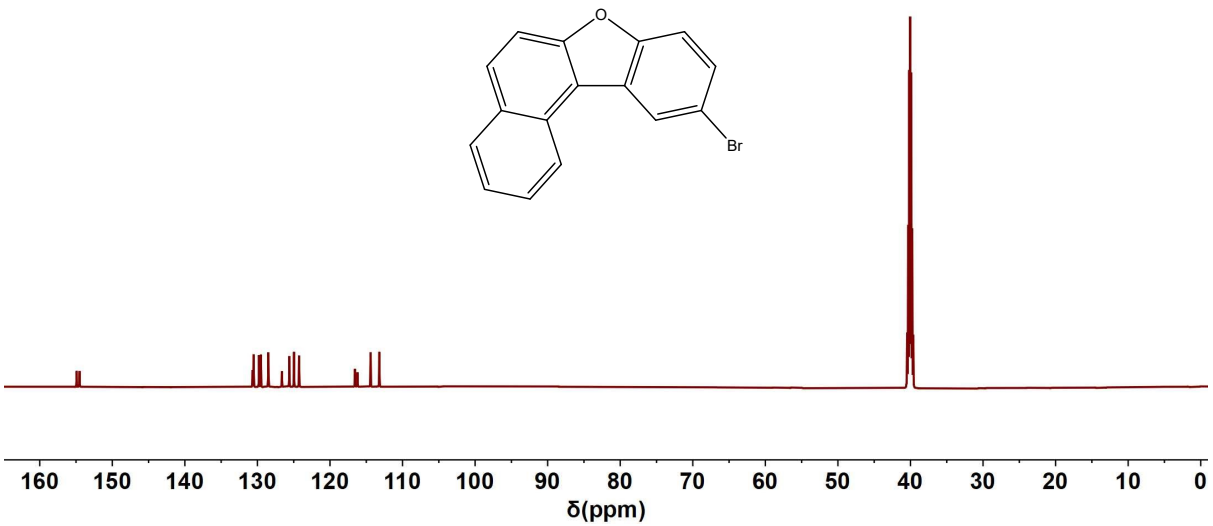

Figure S43. ^{13}C NMR spectrum of 2G in d-DMSO.

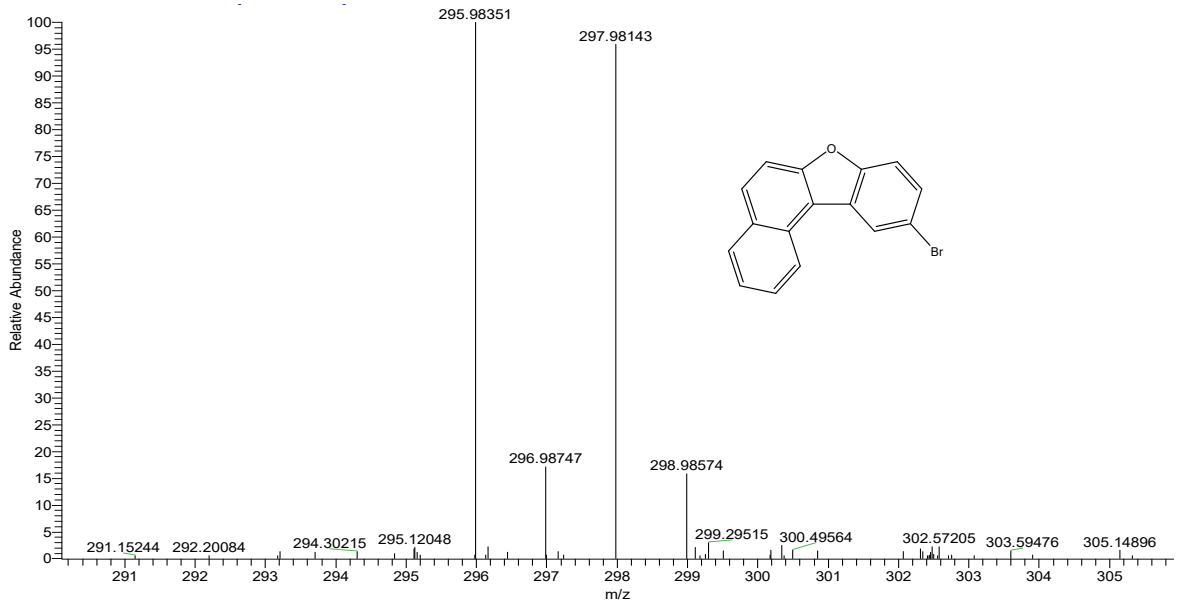

Figure S44. ESI mass spectrum of 2G.

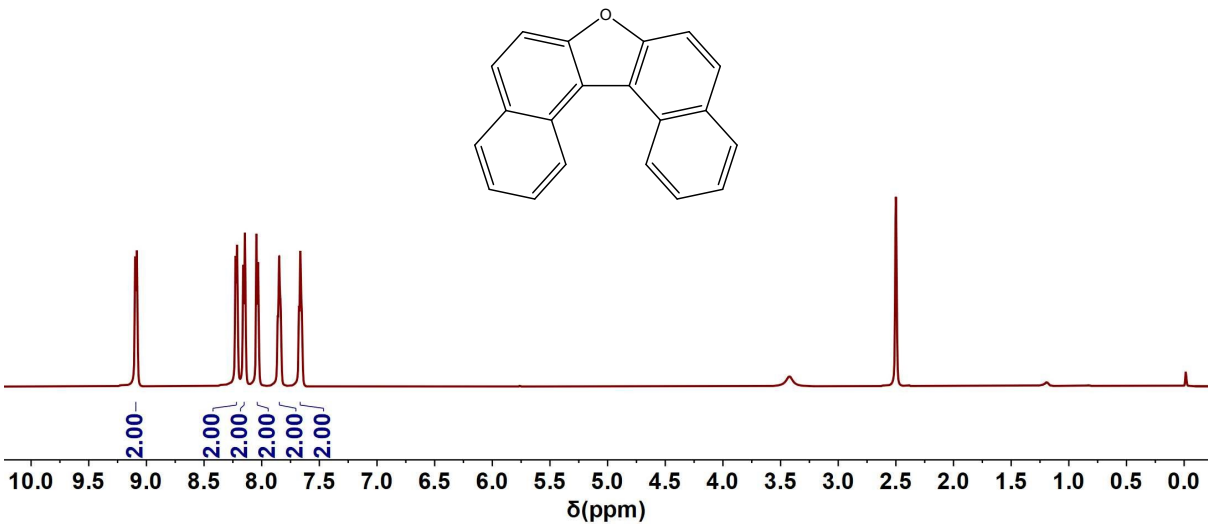

Figure S45. ^{1}H NMR spectrum of 3G in d-DMSO.

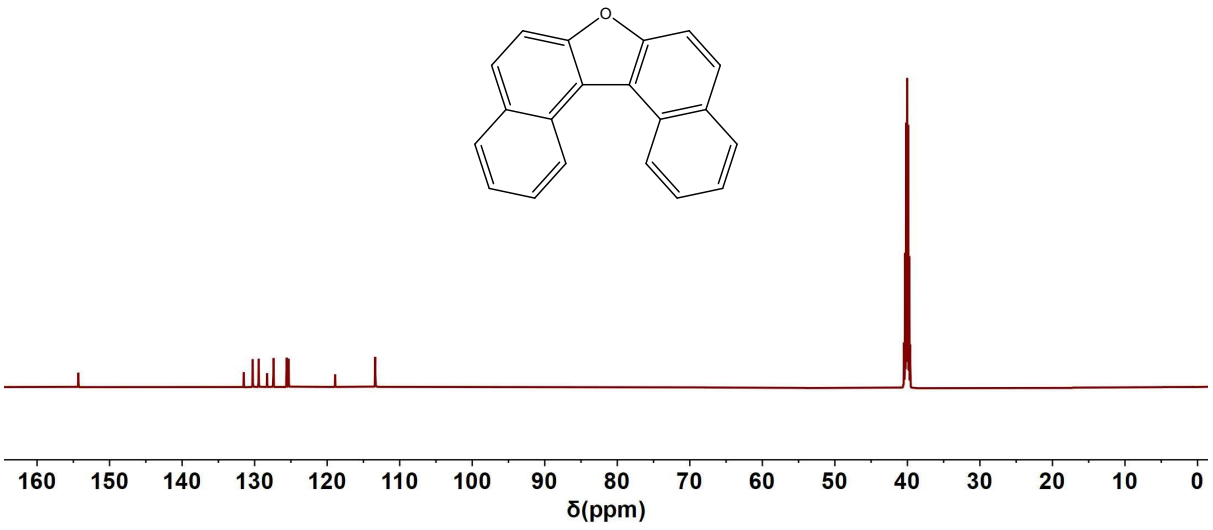

Figure S46. ^{13}C NMR spectrum of 3G in d-DMSO.

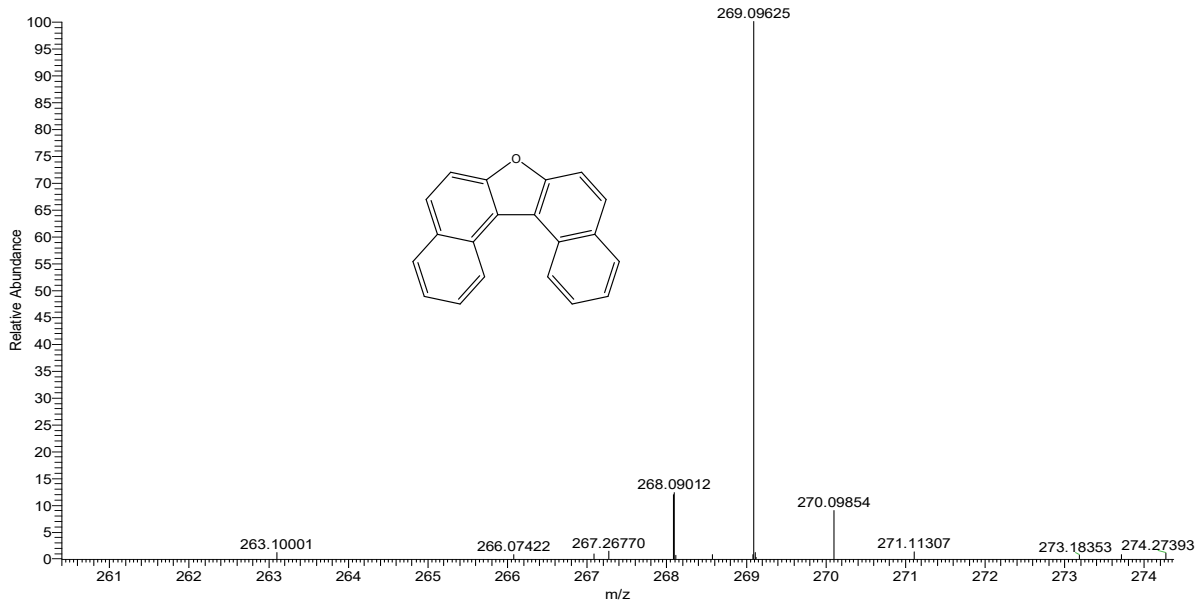

Figure S47. ESI mass spectrum of 3G.

CCDC Depository

Deposition Number 2413907-2413910

Summary of Data - Deposition Number 2413907

Compound Name:

Data Block Name: data_xcl-1_auto

Unit Cell Parameters: a 7.5889(11) b 5.9443(7) c 21.1757(19) P21/c

---

Summary of Data - Deposition Number 2413908

Compound Name:

Data Block Name: data_xc-1-03_auto

Unit Cell Parameters: a 3.98776(8) b 15.4203(3) c 19.0958(3) P212121

Summary of Data - Deposition Number 2413909

Compound Name:

Data Block Name: data_2-3-con_auto

Unit Cell Parameters: a 7.30216(14) b 11.5772(2) c 12.4218(3) P21/c

---

Summary of Data - Deposition Number 2413910

Compound Name:

Data Block Name: data_1

Unit Cell Parameters: a 22.2041(12) b 3.9193(2) c 5.8101(2) Pmn21